Pan-cancer analysis of the extent and consequences of intra-tumor heterogeneity

SUPPLEMENTARY INFORMATION

Noemi Andor, Trevor A. Graham, Marnix Jansen, Li C. Xia, C. Athena Aktipis, Claudia Petritsch, Hanlee P. Ji, Carlo C. Maley

Table of Contents

I. Supplementary Figures

Supplementary Figure 1
Sequencing depth of analyzed TCGA exome sequencing data. Shown is the median and inter-quartile range of sequencing depth in 1,165 exome sequenced tumor samples and matched blood samples, stratified by cancer type. Sequencing depth is shown **(a)** at loci with called somatic SNVs and **(b)** across all sequenced regions.
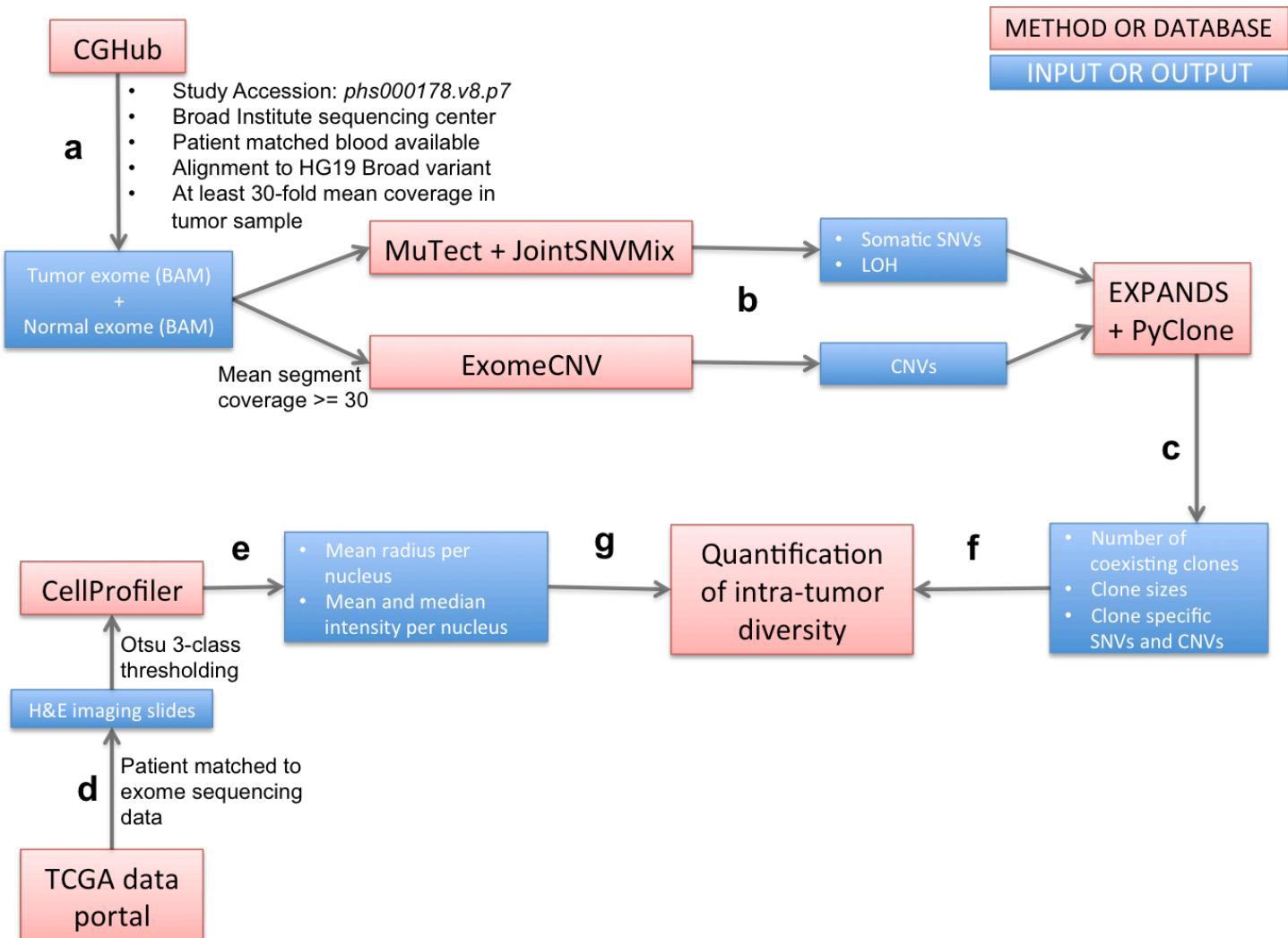
Supplementary Figure 2

Workflow diagram of pan-cancer analysis of ITH.

(a) Raw whole exome sequencing data was downloaded for 1,165 tumor specimens obtained from 1,165 individuals diagnosed with cancer. **(b)** Copy-number segmentation was calculated with ExomeCNV[1]. Somatic point mutations and LOH were inferred with Mutect[2] and JointSNVMix[3]. SNVs outlying autosomes or that cannot be explained by a clone present in 10% or more of the sample (i.e. allele frequency x copy number < 0.1) were excluded. The implemented mutation-calling pipeline is optimized for the quantification of ITH rather than driver mutation discovery. I.e. accurate quantitative assessment of the allelic frequency of a SNV has a high priority. If such assessment is likely imprecise, (due to low sequencing coverage), the SNV is excluded. **(c)** The clonal composition of each tumor was inferred with EXPANDS[4] and PyClone[5] from the detected copy-number segments and SNVs. **(d)** Tumor H&E imaging slides were available for 930 individuals (subset from a). **(e)** Nuclei were detected with CellProfiler[6] software in representative H&E stainings for each specimen and the size and staining intensity of each nucleus was recorded. Intra-tumor diversity measures were quantified for **(f)** genetic and **(g)** histological features. The chosen values for method-parameters or output-thresholds are noted on the arrows. Parameter/output definitions are available in the documentation of the corresponding method.
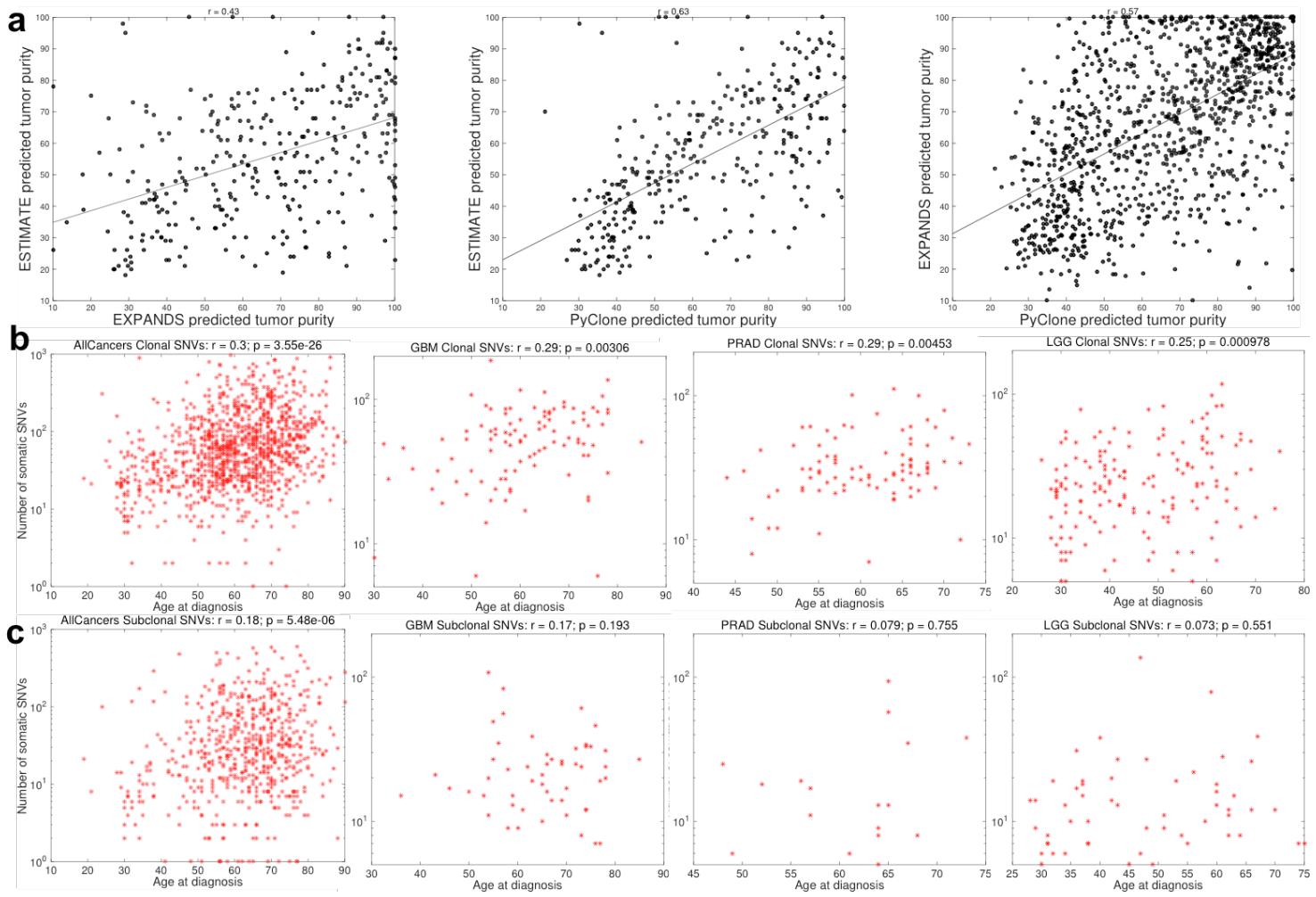
Supplementary Figure 3

Tumor purity predictions, clonal/subclonal SNVs and age at diagnosis. (a) Comparison between PyClone, EXPANDS and ESTIMATE predicted tumor purity. Pairwise correlations between tumor purity predicted based on point mutations and copy number variations (either with EXPANDS or PyClone) and tumor purity predicted based on expression profiling (with ESTIMATE) in 324 TCGA samples (overlap between current study and ESTIMATE publication by Kosuke Yoshihara *et al.*[7]). Left panel: EXPANDS and ESTIMATE (Pearson r=0.43); Central panel: PyClone and ESTIMATE (r=0.63); right panel: PyClone and EXPANDS (r=0.57). ESTIMATE, EXPANDS and PyClone all three predict >99% tumor purity for a subset of the samples. This is particularly frequent among older individuals, possibly because the "normal" (non-cancerous) cells are more likely to have acquired somatic mutations as well. Therefore these non-cancerous, yet mutated cells can be confused with tumor cells. For example, for EXPANDS, the proportion of samples with >99% predicted tumor-cell fraction doubles from 3.1% among individuals younger than 50 years, to 6.2% among individuals above 50 years old. **(b) Age is associated with increasing number of somatic clonal SNVs.** Association between age at diagnosis and number of clonal somatic SNVs is shown for all cancers combined, glioblastoma (GBM), prostate adenocarcinoma (PRAD) and low-grade glioma (LGG). Clonal mutations are defined as SNVs present in minimum 75% of cancer cells. **(c) Correlation between clone number of somatic subclonal SNVs.** Subclonal mutations are defined as SNVs present in maximum 40% of cancer cells. For (b,c) Spearman rank correlation coefficients (r) between age and SNV number is shown along with corresponding p-value on the top of each panel.
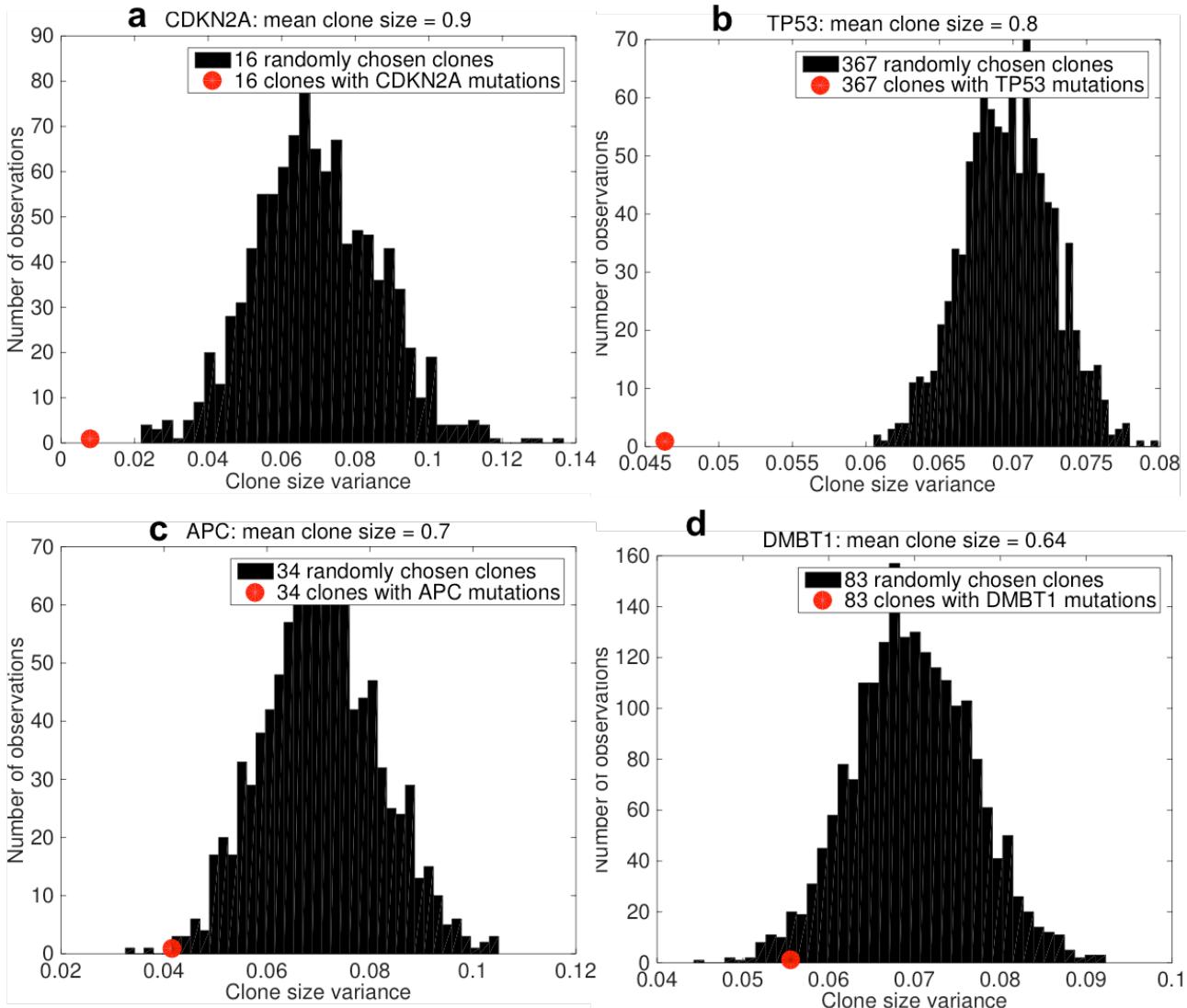
Supplementary Figure 4

CAN-**gene mutations occur in clones of specific,** *CAN*-**gene dependent size-ranges.** The variance in the size of clones with mutations in *CAN*-genes was calculated and compared to the size-variance of clones randomly selected from the cohort of all 5,423 clones detected by EXPANDS across 1,165 tumor samples. Clone sizes were normalized by tumor purity. The clone-size variances of 2,000 randomly selected clone-sets is significantly higher than the size variance of clones harboring **(a)** CDKN2A mutations (t-test: P=0.001), **(b)** TP53 mutations (t-test: P=1. 21E-10), **(c)** APC mutations (t-test: P=0.026) and **(d)** DMBT1 mutations (t-test: P=0.022). The same procedure was performed for all 259 *CAN*-genes.
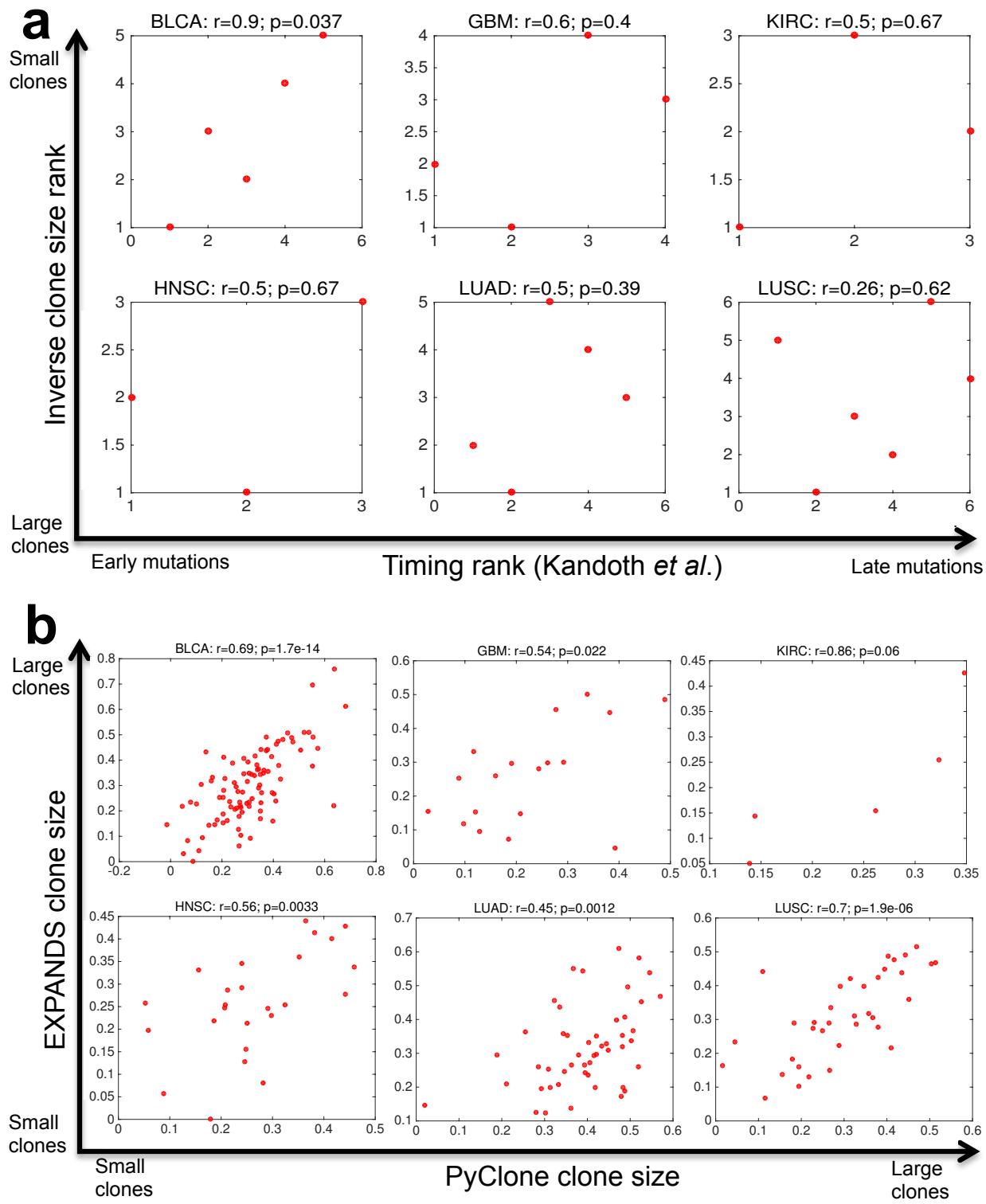
Supplementary Figure 5

Different approaches infer similar sizes for clones with CAN-gene mutations. (a) The size of clones with mutations in cancer driver genes (*CAN*-genes) correlates to the relative order of *CAN*-gene mutations reported by Kandoth *et al*. Correlation between mutation timing rank predicted by Kandoth *et al*. (x-axis) and inverse clone size rank of *CAN*-genes estimated based on EXPANDS results in this study (y-axis). **(b)** The size of clones with cancer driver gene mutations predicted by PyClone (x-axis) and EXPANDS (y-axis). Pearson correlation coefficients (r) are shown.

8

1. TCGA-CF-A47W-01Z-00-DX1
2. TCGA-GU-A42R-01Z-00-DX1
3. TCGA-FD-A3SO-01Z-00-DX1
4. TCGA-G2-A2EK-01Z-00-DX3
5. TCGA-E5-A2PC-01Z-00-DX1
6. TCGA-FD-A5BY-01Z-00-DX1
7. TCGA-GD-A3OS-01Z-00-DX1
8. TCGA-CU-A0YR-01A-01-TS1
9. TCGA-G2-A2EJ-01Z-00-DX4
10. TCGA-GC-A3I6-01Z-00-DX1
11. TCGA-CF-A3MG-01Z-00-DX1
12. TCGA-GV-A40E-01Z-00-DX1
13. TCGA-FJ-A3Z7-01Z-00-DX1
14. TCGA-GV-A3JW-01Z-00-DX1
15. TCGA-FJ-A3ZF-01Z-00-DX1
16. TCGA-C4-A0F0-01Z-00-DX1
17. TCGA-BT-A0YX-01Z-00-DX1

Supplementary Figure 6
Histopathologic evaluation of nuclear ITH measures obtained from automated H&E image analysis. A subset of 17 bladder adenocarcinomas, representative of the full interval of nuclear ITH measured with automated H&E image analysis, was randomly selected. One representative H&E image was examined for each tumor by a histopathologist (MJ) and images were ranked according to ITH in nuclear intensity. Shown are representative regions from each image, sorted according to their histopathologic nuclear ITH ranking (from 1 – least diverse to 17 – most diverse).

9
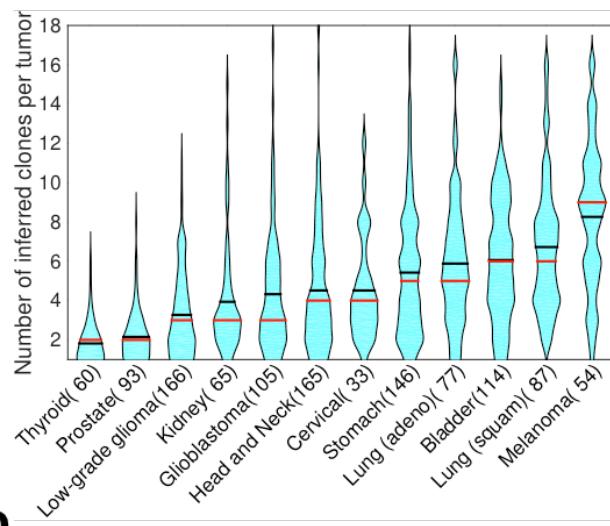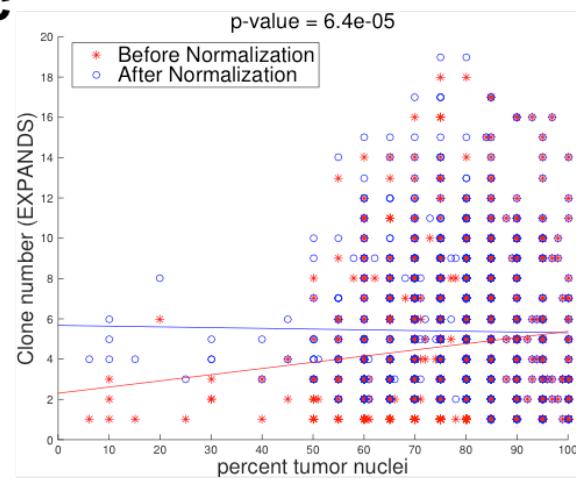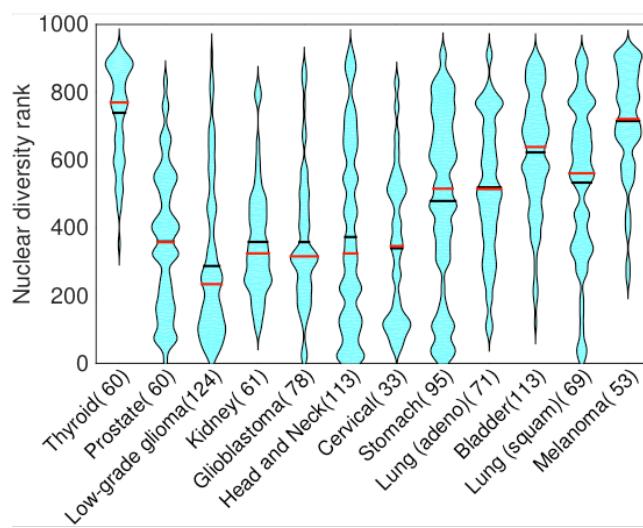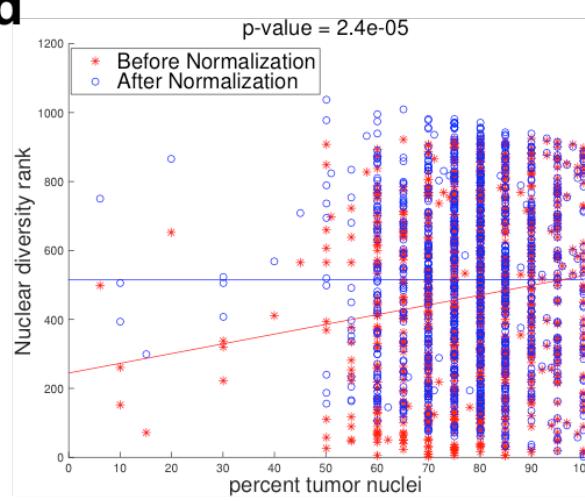
Supplementary Figure 7

ITH distribution across cancers before taking into account tumor purity. Violin plots show clone number **(a)** and nuclear ITH **(b)** within tumor types. Percentage tumor nuclei estimated from histopathological examination correlates to the clone number predicted by EXPANDS (linear regression: P=6.4E-5; coefficient=0.031) **(c),** and to the nuclear ITH inferred from H&E image analysis (P=2.4E-5; coefficient=2.82) **(d),** but not to the clone number predicted by PyClone (P=0.51; data not shown). EXPANDS clone numbers and nuclear ITH measures were therefore normalized by subtracting the tumor-purity associated effects quantified in the linear regression analysis. Tumor-purity normalized clone number and nuclear ITH are shown in main Figs. 1 and 4 respectively.
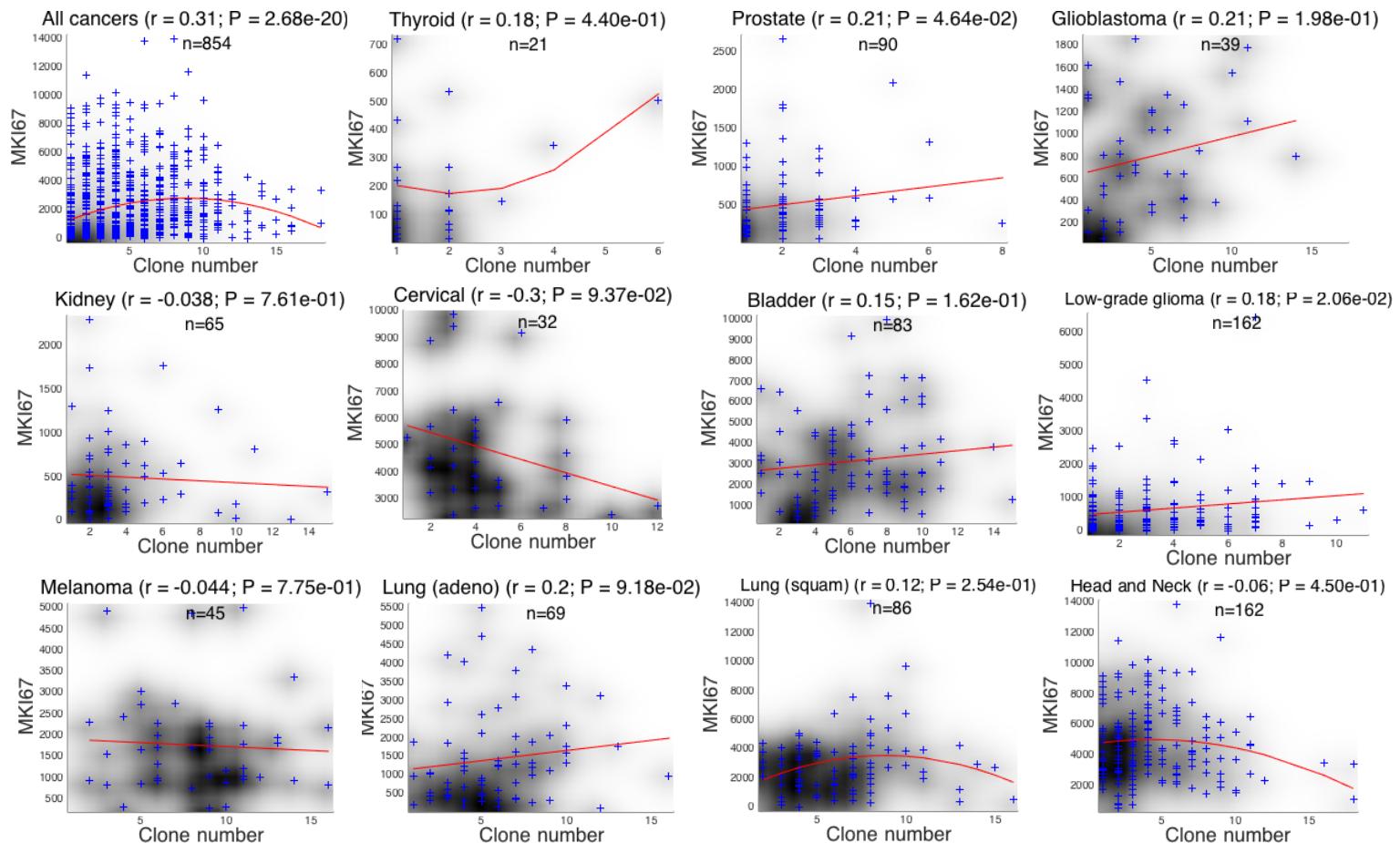
Supplementary Figure 8

Relation between clone number and MKI67 expression. For the majority of cancer types, an increase in clone number is accompanied by an increase in MKI67 expression. For a subset of cancer types, in particular those with a very high absolute proliferation rate (the two squamous carcinomas of head and neck and lung), we observe a non-monotonic relation: tumors with an intermediate number of clones have the highest MKI67 expression, while very heterogeneous tumors (>8 clones) have decreased MKI67 expression. Two alternative models, a linear and a quadratic regression, were fit to model the association between clone number (detected by EXPANDS) and MKI67 mRNA expression. For each cancer type, the model that provided the best fit, as measured by the adjusted R^2, is shown. The Spearman rank correlation coefficient is displayed along with its p-value at the top of each panel. [**Quantification of proliferation rate by MKI67 expression**: *MKI67 mRNA expression was measured by RNA-sequencing, available for 854 tumors (73%). RNA-sequencing data was produced by the University of North Carolina (unc.edu) Cancer Genomic Characterization Center (CGCC) using the Illumina HiSeq 2000 RNA Sequencing Version 2 analysis platform. Expression was calculated at the gene level from RNA-sequencing data using the RSEM software package (RNA-Seq by Expectation-Maximization). RSEM expression estimates were normalized to set the upper quartile count at 1000. The interpreted data (level 3) was downloaded from the TCGA data portal.*]
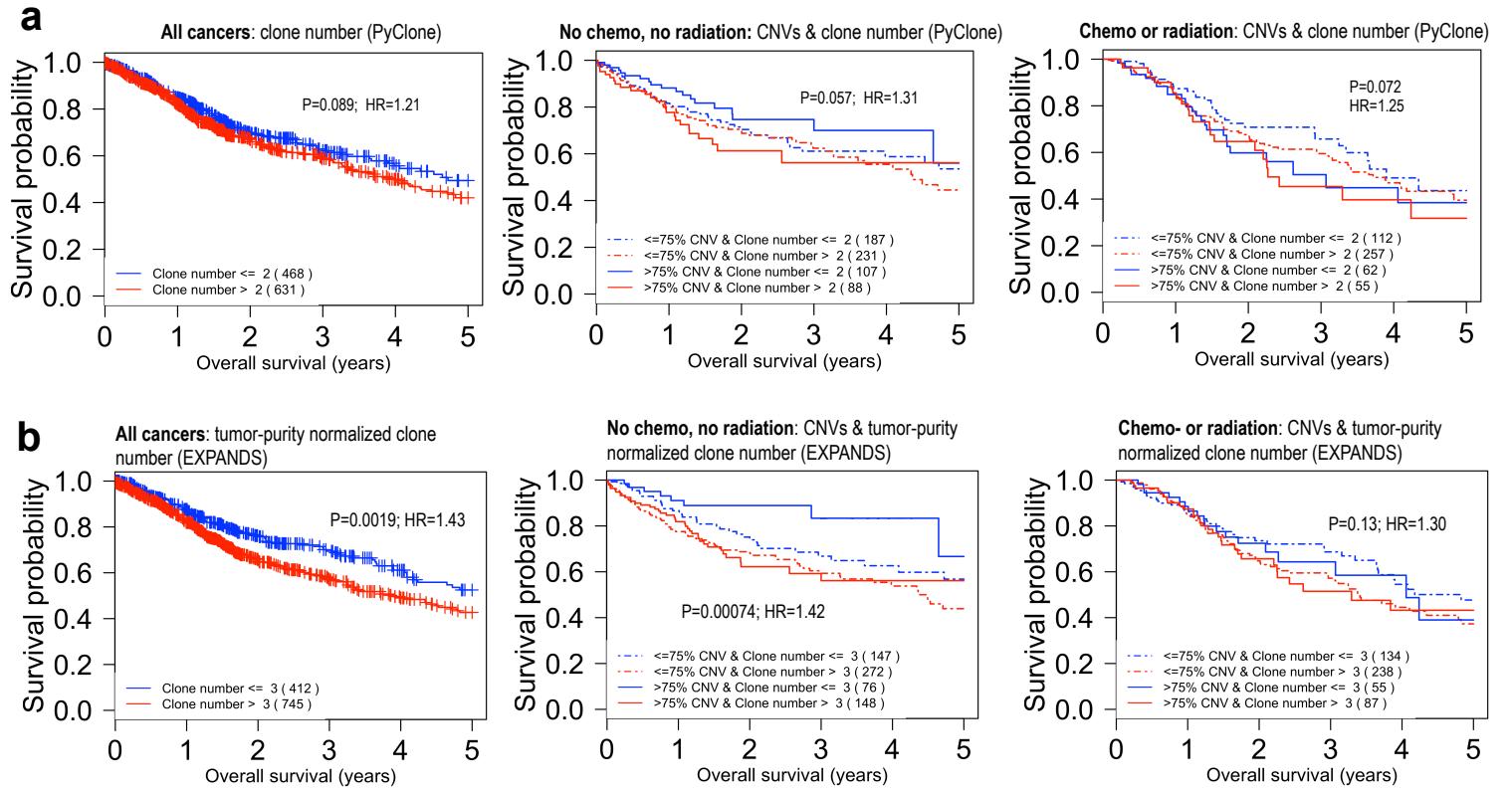
Supplementary Figure 9

Prognostic significance of genetic ITH. (a) PyClone results and **(b)** tumor-purity normalized EXPANDS results (**Supplementary Figure 7**a,c) were used to evaluate the prognostic significance of clone number. **Left panels –** survival curves are stratified by the number of clones detected across 12 tumor types (Log-rank tests: P=0.089, HR=1.21 for PyClone; P=1.9E-3, HR=1.43 for EXPANDS). Individuals who did not undergo chemo- or radiotherapy (**central panels**) and individuals treated with chemo- and/or radiotherapy (**right panels**) are stratified by clone number (red vs. blue lines) and by CNV abundance (dashed vs. continuous lines). In general individuals with few clones in their tumors (blue lines) survive longer than individuals with more clones detected in their tumors (red lines). The prognosis of the patient-group who did not receive chemo- or radiotherapy (central panels) is especially good when these few clones carry a large CNV burden (blue continuous line). This is not the case for individuals treated with chemo- or radiotherapy (right panels).

[The stratification-thresholds for clone number and CNV abundance mark the transition (in clone number and CNV burden respectively), which is accompanied by the greatest change in hazard (see main Fig. 5a-d and Supplementary Fig. 10a). The threshold of 2 used throughout the manuscript for stratification based on clone number is equivalent to a threshold of 3 when accounting for normal cell contamination among tumor samples, i.e. for purity normalized clone numbers].
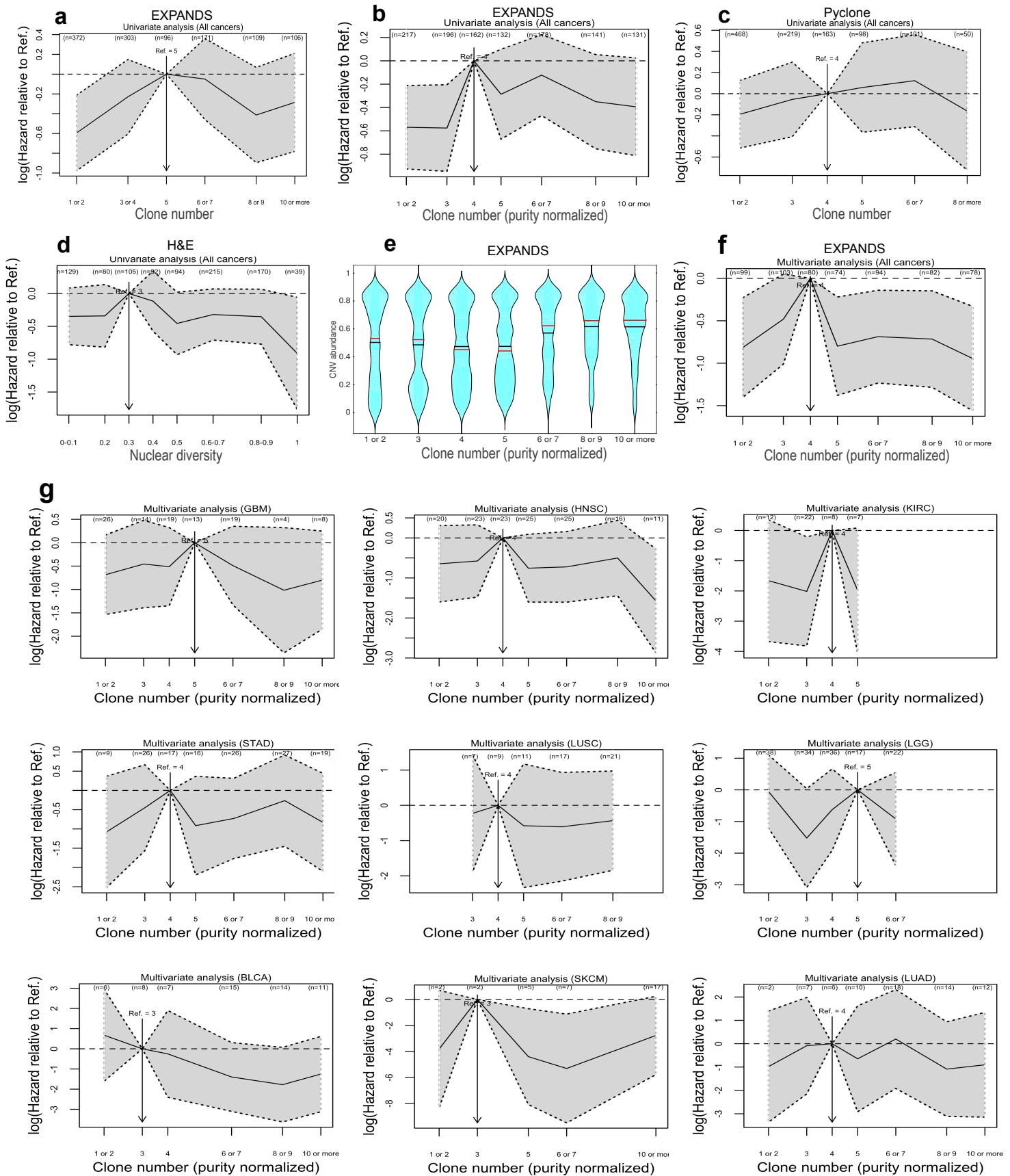
Supplementary Figure 10

Relation of ITH to prognosis and CNV burden. (a-d) Univariate cox models of overall survival across 12 tumor types. The hazard of individuals with low or high ITH (x-axis) is calculated relative to the hazard of individuals with intermediate ITH and is displayed along with 95%-confidence bands. Hazard ratios (y-axis: log-scale) were calculated for alternative measures of ITH: **(a)** clone number inferred by EXPANDS; **(b)** purity normalized clone number (see Supplementary Figure 7) **(c)** clone number inferred by Pyclone and **(d)** nuclear ITH. **(e)** Correlation between the number of clones detected by EXPANDS (x-axis) and the fraction of the tumor-metagenome affected by CNVs (CNV abundance; y-axis; Pearson r=0.17, P=2.1E-9). **(f)** Pan-cancer and **(g)** tumor type specific multivariate Cox models of overall survival. Clone number predicted by EXPANDS was normalized to account for tumor purity and was included as categorical variable into pan-cancer (main Table 1) and tumor-type specific (Supplementary Table 9) multivariate Cox models.
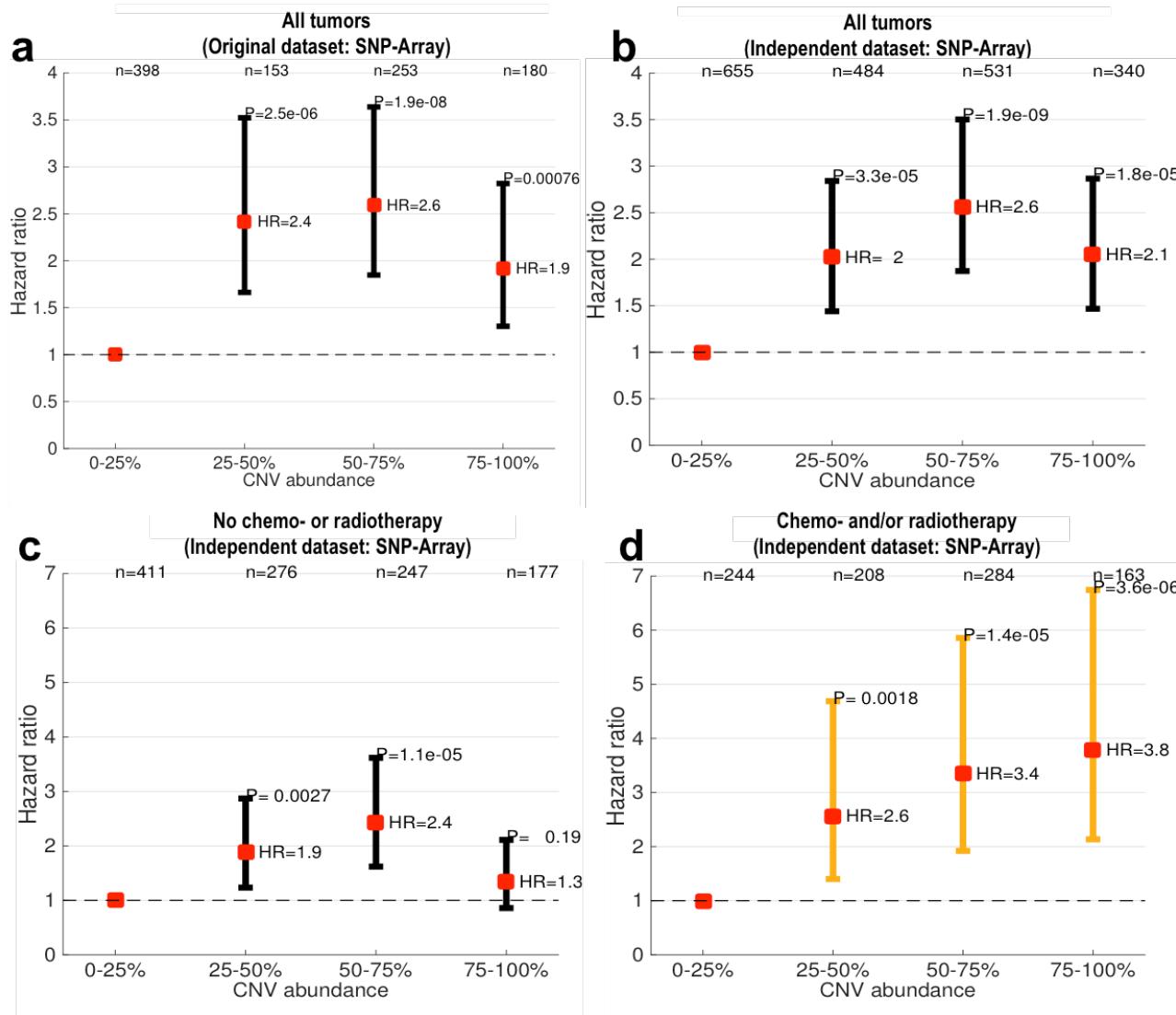
Supplementary Figure 11
Relation between CNV abundance and overall survival based on SNP-array datasets. Hazard ratios as a function of CNV abundance measured on genome-wide SNP arrays (Affymetrix 6.0) in two datasets: **(a)** original tumor-sample set (984 samples overlapping with exome sequenced samples) and **(b-d)** independent dataset (2,010 non-overlapping samples: 74 adrenocortical carcinomas, 989 breast invasive carcinomas, 427 colon adenocarcinomas, 65 kidney chromophobes, 162 rectum adenocarcinomas, 108 sarcomas and 185 ovarian serous cystadenocarcinomas). Independent dataset is further stratified into individuals who did not receive chemo- nor radiotherapy **(c)** and treated individuals **(d).** Among untreated individuals, tumors with intermediate CNV abundance (25-75%) represent the highest risk groups. Among individuals treated with chemo- or radiotherapy, tumors with high CNV abundance (>75%) represent the highest risk group. For every panel, the hazard ratio for each of the upper three CNV abundance quartiles is calculated relative to the hazard of all individuals in the first quartile (0-25% CNV abundance) and displayed along with its 95% confidence interval.

15
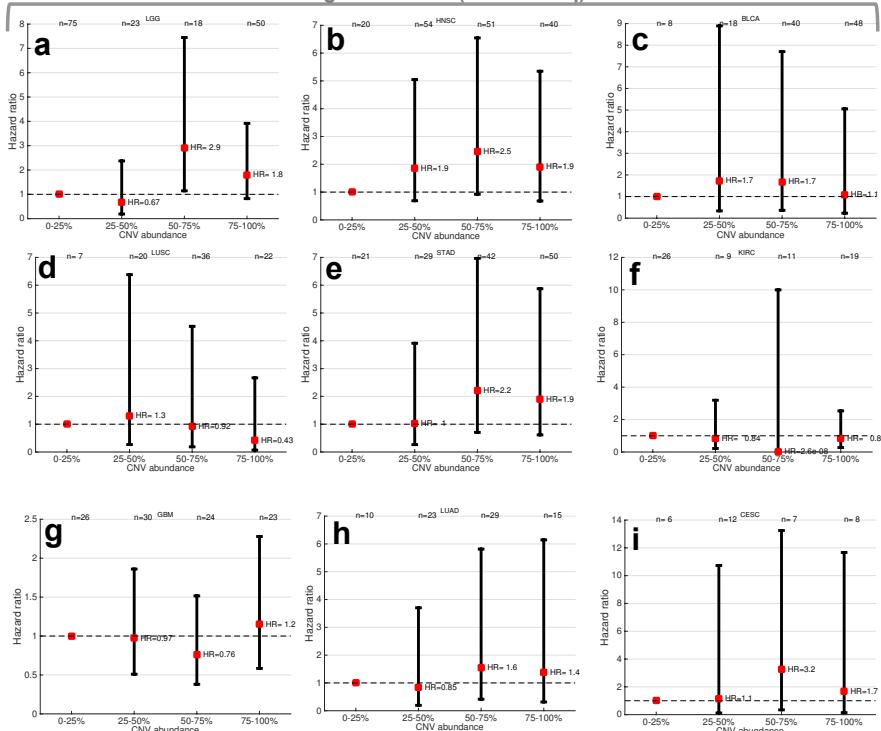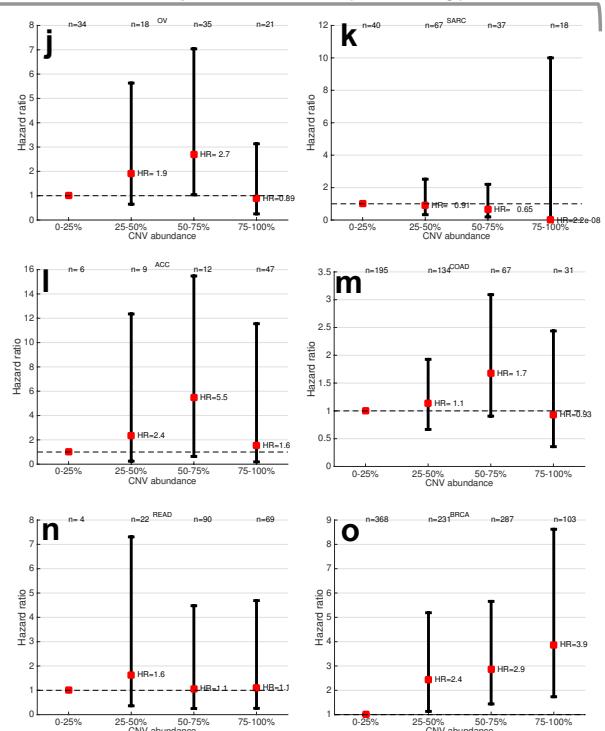
Supplementary Figure 12

Tumors with intermediate CNV burden represent the highest risk-group across most cancer types. Hazard ratios as a function of the % tumor-metagenome affected by CNVs (CNV abundance) in **(a)** low-grade gliomas, **(b)** head and neck cancer**, (c)** bladder cancer, **(d)** lung squamous cell carcinoma, **(e)** stomach cancer, **(f)** kidney cancer, **(g)** glioblastoma, **(h)** lung adenocarcinoma, **(i)** cervical cancer, **(j)** ovarian cancer, **(k)** sarcoma, **(l)** adrenocortical carcinoma, **(m)** colon adenocarcinoma, **(n)** rectum adenocarcinoma and **(o)** breast invasive carcinoma. The hazard ratio and 95% confidence interval associated with each CNV abundance quartile is calculated relative to the hazard of individuals in the first quartile (0-25% CNV abundance), using an univariate Cox model.

16
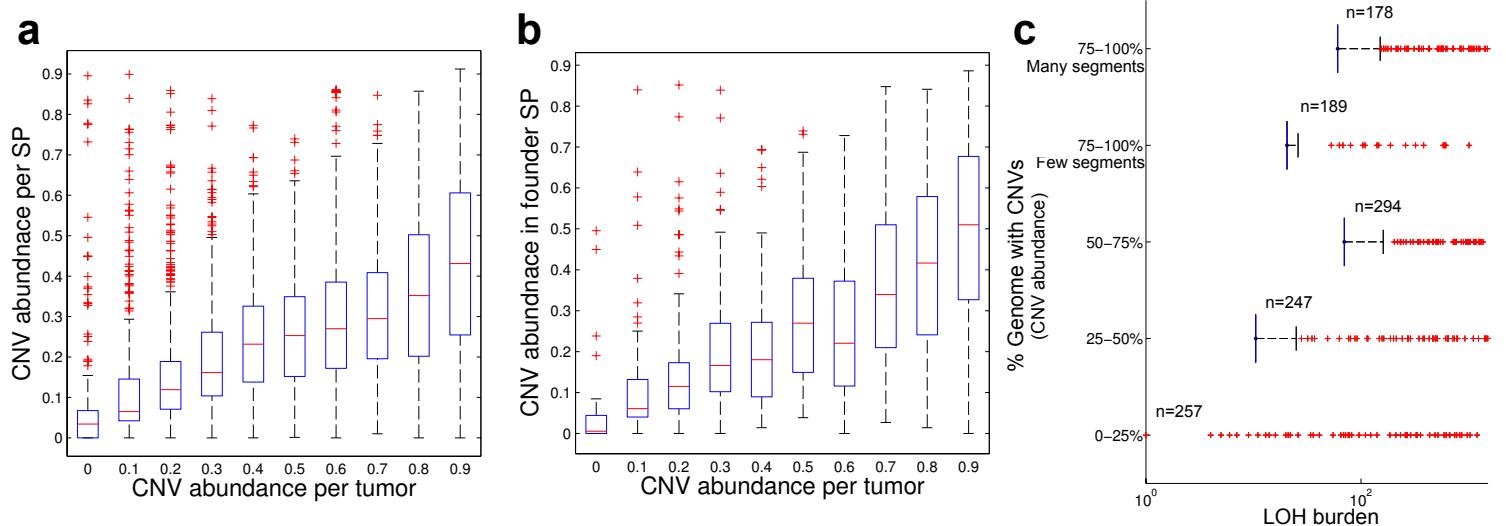
Supplementary Figure 13

Relation between CNV abundance per clone, CNV abundance per tumor-metagenome and LOH incidence. (a) As the fraction of the tumor-metagenome that is affected by CNVs increases, so does the variability in the clonal composition of the tumor. Tumors with >75% of their metagenome affected by CNVs have clones (SPs) with approximately 20-60% of their genome affected by CNVs. **(b)** Founder clones carry similar CNV burden (approximately 30-70% of the genome affected by CNVs). **(c)** To ensure that tumors with >75% of their metagenome affected by CNVs (CNV abundance) were not misclassified and in fact have <25% CNV abundance, we compared loss of heterozygosity (LOH) burden between tumors with different levels of CNV abundance. Mean LOH burden in the >75% CNV abundance tumors was more than two times higher than in tumors with <25% CNV abundance (two-sided Kolmogorov-Smirnov test: P=0.004). LOH burden per tumor (x-axis), is measured as the number of germline SNPs with heterozygous status in the blood sample and homozygous status in the tumor sample. Tumors with >75% CNV abundance are further stratified according to the level of genome fragmentation, using the mode as stratification threshold. Tumors with few segments have fewer LOH than tumors with many segments, but still considerably increased LOH burden as compared to tumors with <25% CNV abundance.

II. Supplementary Notes

Supplementary Note 1: TCGA sequencing data

Raw whole exome sequencing data obtained from tumor samples and matched control samples, on the Illumina sequencing platform, was downloaded from TCGA (Study Accession: *phs000178.v8.p7*) as Binary Alignment/Map (BAM) files.

To facilitate relative comparison of intra-tumor heterogeneity between tumors and cancer types, based on one single sample per tumor, sample selection was designed to obtain high, yet uniformly distributed data quality across the analyzed samples[4]. Inclusion criteria were as follows:

- Availability of sequencing data from matched blood for each tumor sample sequenced.
- Each BAM file obtained from aligning sequencing reads against the HG19 Broad variant (http://www.broadinstitute.org/ftp/pub/seq/references/).
- To reduce inconsistencies between samples and biases related to the sequencing procedure and to preprocessing steps (alignment to the reference genome, indel realignment, base recalibration and duplicate marking), all samples were required to be sequenced by the same sequencing center: the Broad Institute (one out of TCGA's three Genome sequencing centers).
- Tumor samples have at least 30 fold average coverage.
- Absence of neo-adjuvant therapy prior to sample collection.

These criteria applied to 1,165 analyzed tumor samples from 1,165 individuals, which were included in this study. According to TCGA's histological quantifications, the percentage of tumor cells was above 55% in 90% of the analyzed samples. Clinical information associated with the downloaded files is listed in Supplementary Table 7.

Supplementary Note 2: Quantification of genetic ITH by EXPANDS and PyClone

Inference of clonal composition by EXPANDS

EXPANDS[4] version 1.4 was used with default parameters to infer subpopulation composition of tumor samples from sequencing data. EXPANDS is based on the assumption that passenger SNVs accumulate in a cell before a driver event causes a clonal expansion. Consequently, the driver event and all passenger events occurring prior to the driver should be represented in a similar fraction of cells. The model assumes a certain dependency between the number of SNVs detected in the sample and the number of subpopulations expected to co-exist in that sample (e.g. a tumor that harbors only one single somatic mutation cannot consist of two or more genetically distinct populations). Subpopulations (clones) are predicted by clustering SNVs based on their cellular prevalence.

In general, multiple cell-prevalence solutions can explain a given combination of mutated allelic frequency and copy number; for example an SNV with an allele frequency of 0.3, in a ubiquitously diploid region, can either be explained by a homozygous mutation present in 30% of the cells or by a heterozygous mutation present in 60% of the cells. To postpone the final decisions on cellular mutation prevalence and to reduce effects of noise in allele frequencies and copy numbers, entire probability distributions of cellular prevalence are clustered rather than single-value estimates of cellular prevalence. For above example, if the clustering result indicates the presence of a subpopulation at 60% of the sample, while a subpopulation at 30% is not found, then the heterozygous state will be assigned to the SNV. Allele-frequencies (and copy numbers) measured across all detected SNVs can thus help solve ambiguities as to the cellular prevalence and ploidy of individual SNVs.

The accuracy of allele frequencies and copy numbers translate to genomic depth of coverage, base- and mapping qualities as well as consistent experimental conditions for tumor- and control samples. Therefore, the number of clones detected per tumor serves for relative, qualitative comparison of ITH amongst samples sequenced under similar conditions, rather than for absolute quantification of ITH.

Inference of clonal composition by PyClone

The same copy number segments and SNVs used as input for EXPANDS, were used to infer subclonal composition with PyClone. Similar to EXPANDS, PyClone infers the clonal composition of a tumor by grouping SNVs with similar cell-frequencies together. However, inference of the cellular frequency of SNVs is different in that the PyClone model assumes the absence of subclonal CNVs. Therefore copy numbers were rounded to the nearest integer value before using them as PyClone input. In addition the sequencing depth of SNVs detected from TCGA exome sequencing data (Supplementary Figure 1) is marginally sufficient for PyClone, which is specialized to infer clonal structure from deep sequencing data (>100 fold coverage). Lastly,

19

a-priori the PyClone model assumes the sequenced sample is a heterogeneous mixture of cells, which fall into three distinct subpopulations. Therefore, the number of subpopulations detected by PyClone is less dependent on the number of SNVs per sample, than the number of subpopulations detected by EXPANDS (see also above).

In light of these conceptual differences between the two algorithms, PyClone was employed as follows. Let C_E denote the exact copy number of a segment C and C_R the rounded value to the nearest integer copy number. Segments $S_{subclonal} := \{C | \|C_R - C_E\| > t\}$ have a higher likelihood to contain subclonal CNVs. Since PyClone does not offer the possibility to incorporate subclonal CNVs, we excluded clones which were backed up by less than 3 SNVs within segments $S_{clonal} := \{C | \|C_R - C_E\| \le t\}$ from further analysis. As threshold, $t = 0.25$ was chosen. This exclusion rendered 58 tumor samples (5%) with no detectable clones.

We compared the results between EXPANDS and PyClone predictions of subclonal composition:
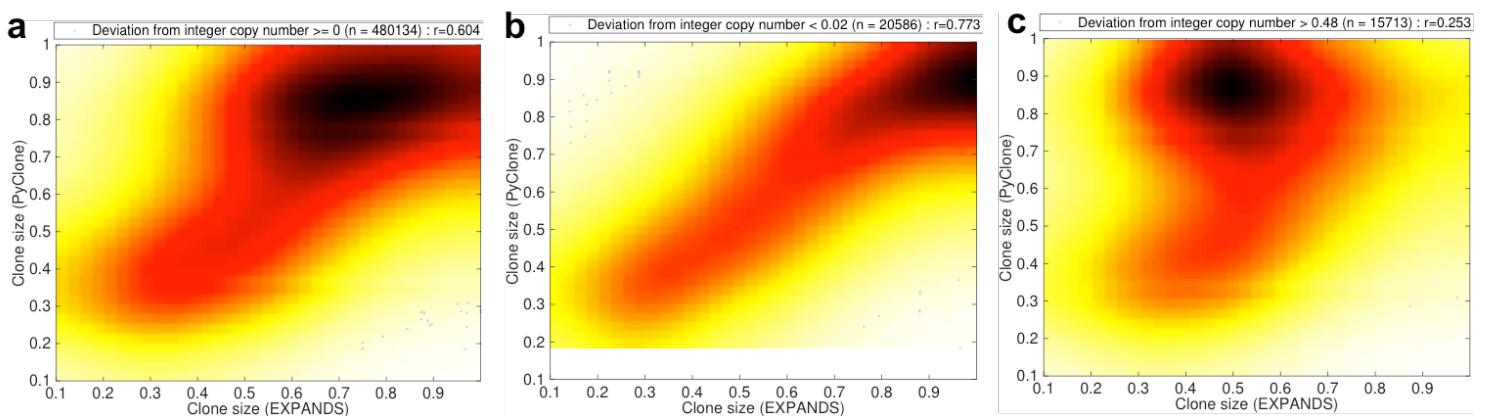
Quantification of genetic ITH by EXPANDS and PyClone. (a) Correlation between cellular frequency of SNVs assigned by EXPANDS (x-axis) and PyClone (y-axis) is shown across all SNVs detected in 1,107 tumor samples (Spearman r=0.61). EXPANDS and PyClone are in considerably better agreement for SNVs embedded within segments for which all tumor cells have similar copy number **(b)** than for SNVs within segments affected by subclonal CNVs **(c)**. This suggests that different a-priori assumptions regarding the presence of subclonal CNVs account for differences between the cellular frequency estimates of the two algorithms.

Relation between genetic ITH and driver mutation incidence

Assuming that each detected clone is the result of a clonal expansion and that each clonal expansion is triggered by a driver mutation, the predicted number of clones also provides a lower boundary estimate of the number of driver events that preceded tumor detection. Compared to the five to eight driver events estimated by epidemiologic studies to be required for the development of solid tumors[8], the number of inferred clones is lower (on average, 4 clones were detected per tumor). This is likely because normal cell contamination reduces clone detection sensitivity and because clone number informs only about the number of clonal expansions that have not yet reached fixation at the time of tumor detection.

20

Supplementary Note 3: Relation between tumor purity and clonal resolution

We addressed the hypothesis that no significant difference in clonal diversity exists between pure and un-pure tumor-samples, i.e. differential clone detection sensitivities between pure and un-pure samples are sufficient to explain differences in clone number.

Let x be the minimum clone size detectable in 100% pure tumors (p:=1). The minimum detectable clone size increases with decreasing tumor purity, from x in 100% pure tumors to $\frac{x}{p}$ in tumors of purity $p<1$. Assuming the distribution of clone sizes in all tumors is the same as it in high-purity tumors, the expected number of clones, n_p, can be estimated as a function of tumor purity p:

$$n_p = |\{s|s \geq \tfrac{x}{p}\}|, \text{ where } x{:}{=}0.25; s \text{ are the sizes of clones detected in high-purity tumors}$$

(>0.9), and p are tumor-purities ranging from 0.25 to 0.9.

We chose x=0.25, because the dependency of detection sensitivity on clone size is negligible for clones present in more than 25% of a high-purity sample (Fig. 2e). Comparing the expected and observed number of clones for variable tumor-purity categories p, suggests that reduced tumor purity is not sufficient to explain the decrease in detected clone number (see panel b in Figure below).
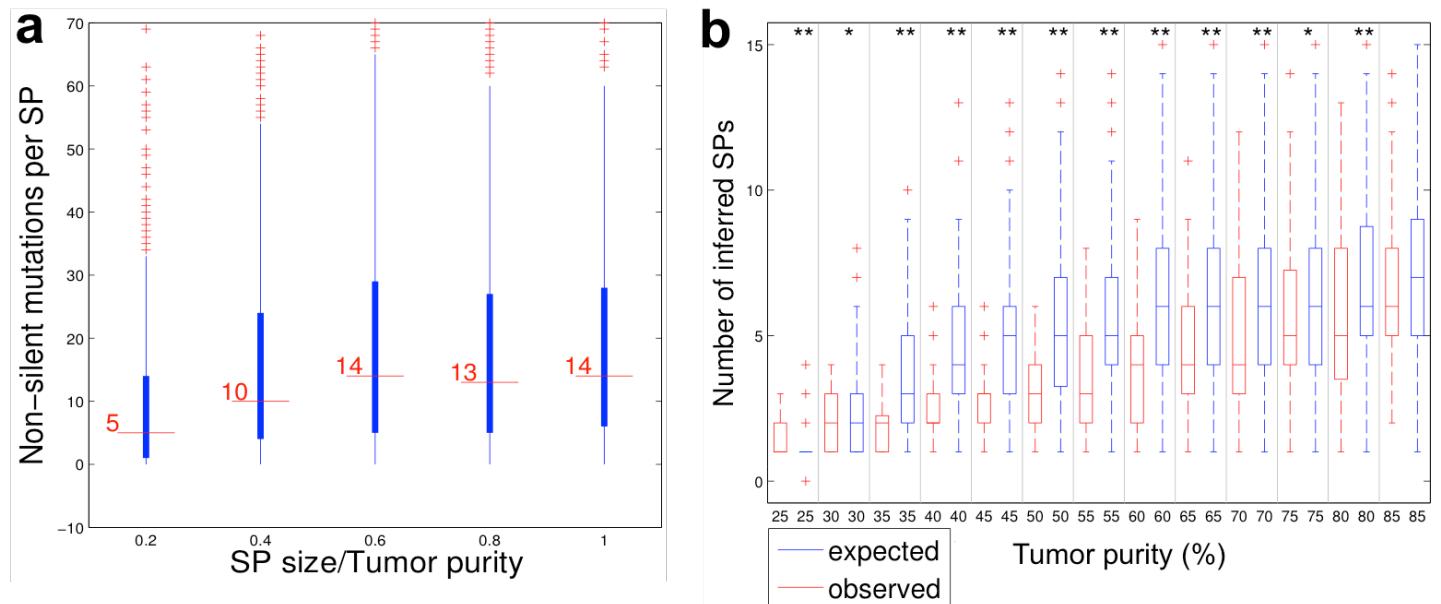
Relation between tumor purity and clonal resolution. (a) Non-silent mutations per clone. Number of non-silent SNVs per clone (SP) is shown for clones of varying size, detected with EXPANDS among 1,165 tumors across 12 cancer types. Reduced incidence of SNVs in small clones is consistent with previous simulation experiments[4] and suggests that small clones will be increasingly missed with decreasing tumor purity. **(b) Expected and observed number of clones detected by EXPANDS in 1,165 samples of differential tumor purity.** Expected and observed clone number was compared within each 5%-tumor-purity category using a two-sample t-test (P<0.05 *; P<0.005 **).

Supplementary Note 4: Quantification of nuclear ITH by H&E image analysis

CellProfiler[6] was used to detect nuclei within H&E images and to measure the size and staining intensity of each detected nucleus. A total of 2,613 representative H&E images were available for 1,064 (91%) of the sequenced tumor samples. For 382 of these images, the lower quartile of pixel intensities was zero (see panel a below). These images were mostly blank and were excluded leaving 2,231 H&E images covering 930 (80%) tumors. Across all images CellProfiler identified an average of 35,000 nuclei per image (see panel b below). For each image I, intra-tumoral nuclear diversity (d) was then quantified from the variability of morphological features f, measured for nuclei in that image:

$$d_f^I = MAD_{Nuclei}(f), \text{ where } f := \{mean\ radius, median\ intensity, mean\ intensity\}$$

We observed a dependency of nuclear diversity features on image quality measures. Each nuclear diversity measure d_f^I was normalized to account for these effects (see panels c-d below). Nuclear diversity for each tumor sample, T, was then calculated as the median normalized nuclear diversity across all images from that tumor:

$$d_f^T = Median_{I \in T}(d_f^I)$$
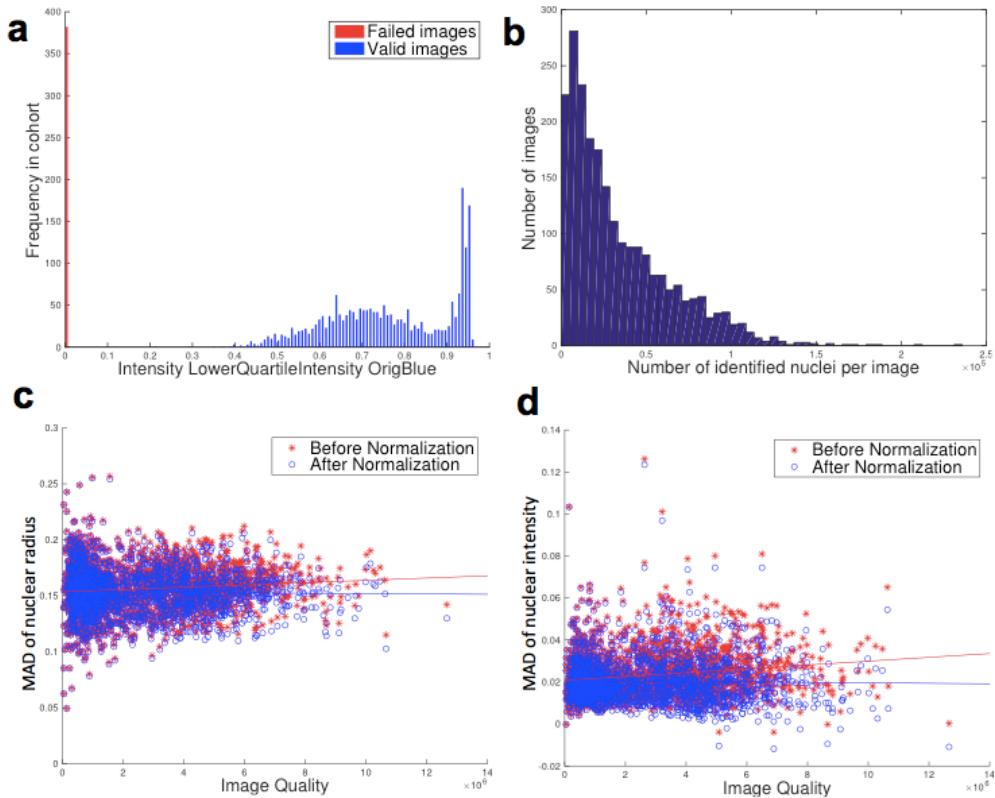
Quantification of nuclear ITH by H&E image analysis. (a) Distribution of the lower quartile of pixel intensities per image measured across 2,613 images. Failed images (red) were excluded from further analysis. **(b)** The number of nuclei identified per each valid image. **(c-d)** Normalization of intra-tumor nuclear diversity measures by image quality. **(c)** Dependence of nuclear size diversity (y-axis) on image quality (x-axis; measured as mean of *AreaOccupied_TotalArea_ThreshBlue* and *AreaOccupied_Perimeter_ThreshBlue*). **(d)** Dependence of nuclear intensity diversity (y-axis) on image quality (x-axis; measured as mean of *Intensity_TotalArea_OrigBlue* and *Intensity_TotalIntensity_OrigRed*). All four image-quality measures are defined in the CellProfiler[6] manual.

Nuclear diversity ranks, R_f^T, were calculated for each tumor, by sorting tumor samples according to the corresponding diversity feature. The final quantification of nuclear diversity (D^T) for each tumor, T, was derived from the median diversity rank:

$$D^T = \frac{Median_f\,(R_f^T)}{\max\,(Median_f\,(R_f^T))}$$

III. Supplementary Tables

Supplementary Table 1

Mean size of clones carrying *CAN*-gene mutations. For each *CAN*-gene *G*, the average size of clones with non-silent mutations in *G* was calculated among all mutated tumors across 12 cancer types. A total of 259 cancer driver genes (*CAN*-genes) were classified according to their SNV occurrence in large-size (upper quartile), medium-size (interquartile range) and small-size (lower quartile) clones and annotated with the functional clustering program DAVID (Supplementary Table 3).

Gene Rank	CAN-Gene	Average clone size (EXPANDS)	Average clone size (PyClone)
1	CDKN1B	86.2	78.4
2	KRAS	85.5	73.8
3	CDKN2A	84.9	76.1
4	VHL	84.8	75.6
5	SDC1	84.3	85.2
6	FSCN1	84.3	63.9
7	CCL2	82.7	83.3
8	TERF1	82.0	72.1
9	EDN3	81.8	71.4
10	BRAF	81.3	75.1
11	TP53	81.1	74.6
12	WNT5A	81.0	71.8
13	NCOA3	80.7	71.5
14	TERT	79.7	84.2
15	PTEN	79.3	72.4
16	PLAT	78.9	76.5
17	GPI	78.6	73.2
18	CADM1	78.4	76.0
19	ITGA2	78.3	61.0
20	CYP1A2	78.0	77.9
21	SOD2	77.8	71.3
22	TAP2	77.7	69.9
23	SERPINA3	77.7	66.5
24	DNTT	77.2	76.2
25	TOP2A	76.8	79.3
26	RB1	76.8	73.5
27	CTNNB1	76.6	72.1
28	CD34	76.6	68.1
29	VIM	76.5	71.3

30	TOP1	76.4	68.9
31	PIK3CA	76.3	69.7
32	CD44	76.1	76.1
34	STAT2	75.8	74.5
33	KRT18	75.6	69.9
35	TSG101	75.3	NA
38	SMAD4	75.3	66.6
37	PIK3CB	75.2	65.3
36	PTGER4	74.9	NA
41	ING1	74.9	67.5
39	RHOA	74.8	66.9
40	NF1	74.7	71.9
42	NBN	74.7	69.7
43	CTSB	74.7	68.1
44	CD82	74.6	74.0
45	SPINT2	74.4	83.0
46	BRCA2	74.3	73.6
47	GFAP	74.3	65.4
48	CCNE1	74.2	78.8
49	TEK	74.1	66.4
50	EGR1	73.8	69.3
51	LAMA5	73.7	68.8
52	AKT1	73.6	77.6
53	TCF7L2	73.6	70.7
54	CP	73.6	66.7
56	ANXA2	73.6	66.1
55	CYP4B1	73.6	62.6
57	XRCC1	73.5	64.2
58	MME	73.4	72.6
59	AXL	73.0	74.0
60	PARP1	73.0	68.6
61	PTCH1	72.9	69.8
62	ALCAM	72.9	64.2
63	FGFR4	72.6	69.0
64	SMAD2	72.5	67.7
65	MET	72.4	68.7
66	MCL1	72.3	66.2
67	HIF1A	72.2	83.0
68	CTTN	72.2	73.8

69	ABCB1	72.2	71.2
71	PPARG	72.1	73.5
70	CDH17	72.1	67.9
72	MPO	72.0	74.3
73	COL18A1	71.8	68.7
76	MUC4	71.7	70.8
75	SLC2A1	71.6	NA
74	CDKN1A	71.6	83.2
77	HPN	71.5	NA
78	ERBB2	71.4	69.1
80	CCKBR	71.4	68.0
79	NRAS	71.4	66.6
81	MUC16	71.3	67.2
82	A2M	71.2	71.9
84	FGFR3	71.0	70.7
83	PTPRC	71.0	66.9
85	PTGS1	71.0	66.6
86	HLA-B	71.0	59.1
87	IL1RN	70.7	70.1
88	PRDM2	70.7	68.1
89	VIP	70.7	64.0
90	CAV1	70.6	78.4
92	CCND3	70.6	69.4
91	SRC	70.6	63.7
93	IGF1R	70.4	73.8
94	MDM2	70.4	68.2
95	NOS3	70.4	64.8
97	VWF	70.3	71.7
98	CLU	70.3	63.7
100	SULT1A1	70.2	75.3
96	DDC	70.1	68.4
99	PRKCA	70.1	68.4
101	STAT3	69.8	72.4
102	MMP14	69.8	66.1
103	NCAM1	69.8	66.1
104	SDHD	69.7	66.1
105	ITGAL	69.5	70.2
106	KRT20	69.4	73.6
107	THBS1	69.3	74.7

108	MAP2K4	69.3	63.0
109	SERPINB5	69.3	60.6
110	DPP4	69.2	78.8
111	CDH1	69.1	69.4
112	SYK	69.0	NA
113	CA9	69.0	72.6
114	TP63	68.9	75.4
115	HSPA4	68.9	70.6
116	AGTR1	68.9	66.5
117	VCAN	68.9	65.2
118	ACTB	68.9	61.6
120	XDH	68.8	62.0
119	MLH1	68.7	74.1
121	JUP	68.7	73.7
122	DLC1	68.7	67.9
123	OGG1	68.6	69.7
124	STAT1	68.6	66.7
125	KRT8	68.6	65.9
126	ABL1	68.6	65.1
127	AHR	68.5	NA
128	LRP1	68.5	70.3
129	KRT5	68.5	68.8
130	HLA-G	68.5	66.3
132	ERBB3	68.4	74.7
131	NOS1	68.4	69.4
133	FLT4	68.4	63.9
135	TSHR	68.4	63.0
134	MTHFR	68.3	64.6
136	ERCC2	68.1	77.6
137	EGF	68.1	72.1
139	KDR	68.1	70.6
138	EPHA2	68.1	62.8
140	SMARCA4	68.0	72.3
141	EGFR	68.0	65.1
142	CYP1A1	67.8	NA
143	ANGPT2	67.7	67.6
144	FLT1	67.7	66.1
145	MKI67	67.6	72.6
146	APC	67.6	65.1

147	HSPA1A	67.5	66.1
148	DAPK1	67.4	71.1
149	PKHD1	67.4	69.6
150	NOTCH1	67.4	63.8
151	NTRK1	67.3	69.8
154	EPHB4	67.3	68.9
152	DPYD	67.3	67.8
153	PTHLH	67.3	58.6
155	MMP11	67.2	74.5
156	IL4R	67.2	68.8
157	LZTS1	67.2	68.4
158	BUB1	67.2	53.0
159	TNF	66.9	77.6
160	MMP9	66.8	68.3
161	ENPEP	66.7	NA
162	MTA1	66.7	76.1
163	ETS2	66.7	68.9
164	CEACAM5	66.7	64.9
165	AFP	66.6	NA
166	ABCC1	66.6	65.8
167	DCC	66.4	67.0
168	GLI1	66.3	70.5
169	NAT2	66.3	69.5
170	SART3	66.3	61.1
171	PGR	66.1	59.4
172	REG4	66.0	63.0
173	ITGB2	65.9	68.2
174	ANPEP	65.8	72.3
177	CDH3	65.8	68.0
176	MYB	65.8	67.0
175	HSPG2	65.8	65.5
178	EDNRB	65.6	73.2
179	SLC2A3	65.5	75.2
180	CTSD	65.5	68.3
182	APAF1	65.4	NA
181	ENO2	65.3	80.3
183	PIK3CG	65.3	75.5
184	GNAS	65.3	63.3
185	MAPK1	65.2	71.8

186	DBC1	65.2	68.7
187	MVP	65.1	65.7
188	WT1	65.1	58.6
189	KRT7	65.1	58.0
190	MUC6	65.0	60.1
191	PTGS2	64.7	69.5
192	CDC73	64.6	NA
193	TSC1	64.6	68.6
194	MUC2	64.6	66.1
195	CHFR	64.4	NA
196	RET	64.4	70.2
197	IL15	64.4	66.3
198	TRPM1	64.3	68.7
199	PLAUR	64.3	60.0
200	DMBT1	64.1	65.2
201	XRCC5	64.0	66.1
202	FGFR2	64.0	66.0
203	UMPS	63.9	NA
204	NOS2	63.8	69.4
205	HDC	63.8	65.3
206	TG	63.8	65.1
207	MT3	63.8	64.2
208	MC2R	63.7	75.4
209	HGF	63.7	58.6
210	ANGPT1	63.6	61.2
211	MSH6	63.4	59.0
212	TGFB1	63.3	66.7
213	MUC5B	63.2	74.0
214	FAP	63.2	66.5
215	VCAM1	63.1	65.5
216	ENPP2	63.0	72.8
217	HSP90AA1	62.9	73.8
218	GSTP1	62.8	NA
219	CD86	62.6	72.3
220	NQO1	62.5	59.4
221	BAX	62.3	70.9
222	VEGFA	62.2	59.7
223	NRP1	62.2	58.5
224	CD55	62.1	NA

225	BRCA1	62.1	68.5
226	IGHG3	62.1	62.0
227	MUC3A	62.0	58.8
228	RUNX2	61.9	NA
229	ZBTB16	61.8	69.8
230	ESR2	61.7	70.1
231	FASN	61.7	66.0
232	INSR	61.7	61.7
233	FGF2	61.3	NA
234	HLA-A	60.9	60.5
235	MMP2	60.8	66.0
236	KCNH2	60.6	55.9
237	LTF	60.5	67.6
238	EZH2	60.4	71.8
239	RARB	59.6	70.4
240	TFAP2A	59.5	61.2
241	HSP90B1	59.3	60.9
242	CDC25A	59.3	57.7
243	CHEK2	59.1	60.9
244	CDC25B	59.0	66.8
245	ICAM1	58.3	61.8
246	BMP6	57.7	62.5
247	MYC	57.7	59.2
248	XPA	57.3	NA
249	EPO	57.1	88.8
250	TP73	56.7	71.6
251	NFKB1	56.7	64.0
252	HMMR	56.6	NA
253	MUTYH	54.9	53.6
254	GJA1	53.8	71.6
255	MUC5AC	52.5	52.3
256	FOLH1	52.4	58.4
257	PLK1	51.9	65.9
258	TNFRSF1A	51.0	55.1
259	MAD2L1	38.8	31.9

Supplementary Table 2
Prognostic significance of genetic ITH and cell-proliferation rate across cancers. P-values and hazard ratios from univariate Cox models. P-values below 0.05 are marked blue. The magnitude of the hazard ratio is color-coded (yellow: favorable outcome; red: poor outcome; gray: moderate effect). Where variables did not satisfy the proportionality assumption for the Cox model (P<0.05), the corresponding hazard ratios are flagged (*). Two clinical endpoints are shown: **(a)** overall survival and **(b)** progression-free survival. NA:= not available.

a

		Progression Index (EXPANDS)	Progression Index (PyClone)	Clone number (EXPANDS)	Purity normalized Clone number (EXPANDS)	Clone number (PyClone)	Nuclear diversity rank (H&E)	MKI67
All cancers (including PRAD & THCA)	p-value (Cox)	3.17E-07	0.01	0.08	0.23	0.27	0.09	1.40E-04
	corrected p-value (Cox)	2.22E-06	0.02	0.53	0.82	0.77	0.46	1.68E-03
	hazard ratio (Cox)	2.86	1.67	1.64	1.43	1.36	0.70	3.49*
	# samples	1157	1157	1157	1157	1099	924	852
STAD	p-value (Cox)	0.36	0.63	0.73	0.78	0.85	0.26	NA
	corrected p-value (Cox)	0.62	0.68	0.94	0.84	1.00	0.51	NA
	hazard ratio (Cox)	1.85	1.36	0.75	0.80	0.86	0.43	NA
	# samples	142	142	142	142	141	92	NA
GBM	p-value (Cox)	0.04	1.62E-03	0.55	0.71	0.03	0.45	0.55
	corrected p-value (Cox)	0.11	0.01	0.92	0.82	0.31	0.55	0.68
	hazard ratio (Cox)	2.27	3.84	1.44	1.27	2.72	1.50	1.40*
	# samples	103	103	103	103	101	77	39
LGG	p-value (Cox)	1.60E-03	0.24	0.50	0.30	0.60	0.14	0.01
	corrected p-value (Cox)	0.01	0.43	0.92	0.82	1.00	0.46	0.02
	hazard ratio (Cox)	4.04	1.77	0.58	0.38	0.67	2.99	10.52
	# samples	166	166	166	166	145	124	162
Glioma (GBM+LGG)	p-value (Cox)	2.28E-09	1.42E-05	0.03	0.55	0.04	0.01	4.73E-03
	corrected p-value (Cox)	3.20E-08	1.98E-04	0.45	0.82	0.31	0.16	0.02
	hazard ratio (Cox)	6.70	4.04	3.25	1.44	2.34	2.76	6.49
	# samples	269	269	269	269	246	201	201
KIRC	p-value (Cox)	0.02	0.04	0.67	0.69	0.58	0.40	0.26
	corrected p-value (Cox)	0.06	0.13	0.93	0.82	1.00	0.55	0.52
	hazard ratio (Cox)	5.92	3.48	0.55	0.58	0.57	0.40*	3.53
	# samples	65	65	65	65	60	61	65
HNSC	p-value (Cox)	0.44	0.35	0.98	0.98	0.07	0.64	0.88
	corrected p-value (Cox)	0.68	0.55	1.00	0.98	0.35	0.69	0.88
	hazard ratio (Cox)	1.36	1.40	0.98	1.02	0.29	0.80	1.11
	# samples	165	165	165	165	164	113	162
LUAD	p-value (Cox)	0.72	0.05	0.22	0.17	0.93	0.27	0.18
	corrected p-value (Cox)	0.92	0.13	0.78	0.82	1.00	0.51	0.50
	hazard ratio (Cox)	0.78	0.32	0.31	0.26	0.93*	0.40	3.24
	# samples	77	77	77	77	77	71	69
BLCA	p-value (Cox)	0.35	0.25	0.58	0.68	0.28	0.18	0.34
	corrected p-value (Cox)	0.62	0.43	0.92	0.82	0.77	0.46	0.59
	hazard ratio (Cox)	0.53	0.51	0.64	0.72	0.40	0.36*	2.69*
	# samples	114	114	114	114	112	113	83
LUSC	p-value (Cox)	0.93	0.49	0.12	0.09	0.80	0.43	0.56
	corrected p-value (Cox)	0.93	0.60	0.54	0.82	1.00	0.55	0.68
	hazard ratio (Cox)	1.07*	0.61	0.17	0.14	1.28	0.48	2.51
	# samples	85	85	85	85	84	67	84
SKCM	p-value (Cox)	0.93	0.51	0.31	0.29	0.95	0.80	0.42
	corrected p-value (Cox)	0.93	0.60	0.87	0.82	1.00	0.80	0.62
	hazard ratio (Cox)	1.10	0.52	0.34	0.33	1.06	1.25	0.33
	# samples	54	54	54	54	53	53	45
CESC	p-value (Cox)	0.27	0.11	0.59	0.40	0.67	0.15	0.85
	corrected p-value (Cox)	0.62	0.25	0.92	0.82	1.00	0.46	0.88
	hazard ratio (Cox)	0.37	0.21	0.47	0.28	0.58	0.18	0.80
	# samples	33	33	33	33	33	33	32

31

b

		Progression Index (EXPANDS)	Progression Index (PyClone)	Clone number (EXPANDS)	Purity normalized Clone number (EXPANDS)	Clone number (PyClone)	Nuclear diversity rank (H&E)	MKI67
All cancers (including PRAD & THCA)	p-value (Cox)	1.19E-03	0.32	0.42	0.67	0.24	0.01	0.01
	corrected p-value (Cox)	0.01	0.56	0.83	0.85	0.71	0.08	0.04
	hazard ratio (Cox)	1.81	1.18	1.22	1.12	1.34	0.58	2.24
	# samples	1157	1157	1157	1157	1099	924	852
STAD	p-value (Cox)	0.71	0.65	0.23	0.25	0.48	0.03	NA
	corrected p-value (Cox)	0.93	0.79	0.83	0.85	0.74	0.13	NA
	hazard ratio (Cox)	1.24	0.79	0.38	0.41	0.60	0.24	NA
	# samples	142	142	142	142	141	92	NA
GBM	p-value (Cox)	0.26	0.17	0.77	0.51	0.25	0.99	0.72
	corrected p-value (Cox)	0.62	0.53	0.97	0.85	0.71	0.99	0.78
	hazard ratio (Cox)	1.53	1.79	0.85	0.68	1.69	0.99	1.23
	# samples	103	103	103	103	101	77	39
LGG	p-value (Cox)	0.07	0.63	0.25	0.17	0.44	0.12	0.15
	corrected p-value (Cox)	0.35	0.79	0.83	0.85	0.74	0.35	0.40
	hazard ratio (Cox)	1.99	1.23	0.48	0.37	0.62	2.50	2.99
	# samples	166	166	166	166	145	124	162
Glioma (GBM+LGG)	p-value (Cox)	3.21E-06	4.41E-03	0.25	0.74	0.25	0.02	0.09
	corrected p-value (Cox)	4.49E-05	0.06	0.83	0.86	0.71	0.11	0.38
	hazard ratio (Cox)	3.78	2.32	1.76	0.83	1.55	2.39	2.82
	# samples	269	269	269	269	246	201	201
KIRC	p-value (Cox)	0.14	0.08	0.56	0.63	0.36	0.62	0.31
	corrected p-value (Cox)	0.48	0.49	0.83	0.85	0.74	0.87	0.47
	hazard ratio (Cox)	2.82	2.51	0.50	0.57	0.41	0.61	2.59
	# samples	65	65	65	65	60	61	65
HNSC	p-value (Cox)	0.79	0.68	0.96	0.94	0.23	0.72	0.52
	corrected p-value (Cox)	0.93	0.79	1.00	0.94	0.71	0.91	0.62
	hazard ratio (Cox)	1.10	1.14	0.97	1.06	0.50	1.18	1.47
	# samples	165	165	165	165	164	113	162
LUAD	p-value (Cox)	1.00	0.27	0.55	0.53	0.85	0.93	0.38
	corrected p-value (Cox)	1.00	0.55	0.83	0.85	0.94	0.99	0.51
	hazard ratio (Cox)	1.00	0.59	0.66	0.64	0.88 *	1.06	1.87
	# samples	77	77	77	77	77	71	69
BLCA	p-value (Cox)	0.35	0.24	0.48	0.55	0.19	0.20	0.19
	corrected p-value (Cox)	0.70	0.55	0.83	0.85	0.71	0.40	0.40
	hazard ratio (Cox)	0.55	0.53	0.58	0.64	0.33	0.39 *	3.49 *
	# samples	114	114	114	114	112	113	83
LUSC	p-value (Cox)	0.40	0.92	0.92	0.80	0.65	0.10	0.23
	corrected p-value (Cox)	0.70	0.92	1.00	0.86	0.86	0.35	0.40
	hazard ratio (Cox)	2.00 *	0.93	0.91	0.80	1.46	0.25	5.26
	# samples	85	85	85	85	84	67	84
SKCM	p-value (Cox)	0.45	0.19	0.31	0.27	0.87	0.84	0.24
	corrected p-value (Cox)	0.70	0.53	0.83	0.85	0.94	0.98	0.40
	hazard ratio (Cox)	0.46	0.29	0.35	0.33	0.87	1.19	0.18
	# samples	54	54	54	54	53	53	45
CESC	p-value (Cox)	0.27	0.11	0.59	0.40	0.67	0.15	0.85
	corrected p-value (Cox)	0.62	0.49	0.83	0.85	0.86	0.35	0.85
	hazard ratio (Cox)	0.37	0.21	0.47	0.28	0.58	0.18	0.80
	# samples	33	33	33	33	33	33	32

Supplementary Table 3

Annotation clustering of *CAN*-genes stratified by mutated clone sizes. Mutually exclusive pathways (from BIOCARTA and KEGG databases: prefix *h_telpathway, hsa*), gene ontologies (prefix *GO*) and protein domains (INTERPRO database: prefix *IPR*) enriched either among cancer driver genes (*CAN*-genes) harboring mutations in large clones (upper quartile) or among *CAN*-genes with mutations in small- and medium-sized clones (lower three quartiles). The top-20 enriched entities[9,10] are shown for each of the two clone size categories.

Enriched Term	*CAN*-gene size category	Gene count	*P*-Value	FDR
hsa05200:Pathways in cancer	Large	23	1.92E-14	2.10E-11
hsa05212:Pancreatic cancer	Large	11	7.26E-10	7.93E-07
hsa05210:Colorectal cancer	Large	11	3.44E-09	3.76E-06
GO:0008285~negative regulation of cell proliferation	Large	14	7.15E-09	1.19E-05
GO:0007568~aging	Large	9	3.47E-08	5.78E-05
hsa05222:Small cell lung cancer	Large	10	5.89E-08	6.43E-05
GO:0040008~regulation of growth	Large	12	3.58E-07	0.001
GO:0042493~response to drug	Large	10	5.56E-07	0.001
GO:0001666~response to hypoxia	Large	8	2.50E-06	0.004
GO:0070482~response to oxygen levels	Large	8	3.51E-06	0.006
GO:0001889~liver development	Large	6	4.16E-06	0.007
GO:0007050~cell cycle arrest	Large	7	7.32E-06	0.012201
GO:0007569~cell aging	Large	5	1.48E-05	0.024682
GO:0051130~positive regulation of cellular component organization	Large	8	1.81E-05	0.030107
GO:0008134~transcription factor binding	Large	12	2.29E-05	0.030181
GO:0008283~cell proliferation	Large	11	2.61E-05	0.043541
hsa05211:Renal cell carcinoma	Large	7	4.26E-05	0.04655
h_telPathway:Telomeres, Telomerase, Cellular Aging, and Immortality	Large	6	7.50E-05	0.08685
hsa04510:Focal adhesion	Large	10	8.64E-05	0.094363
IPR001357:BRCT	Large	4	1.03E-04	0.134645
GO:0044093~positive regulation of molecular function	Small, Medium	38	5.90E-15	1.04E-11
IPR008266:Tyrosine protein kinase, active site	Small, Medium	17	1.67E-14	2.47E-11
GO:0043085~positive regulation of catalytic activity	Small, Medium	35	3.18E-14	5.63E-11
GO:0004714~transmembrane receptor protein tyrosine kinase activity	Small, Medium	15	3.01E-13	4.35E-10
IPR001245:Tyrosine protein kinase	Small, Medium	17	3.97E-13	5.84E-10
GO:0007169~transmembrane receptor protein tyrosine kinase signaling pathway	Small, Medium	23	5.57E-13	9.87E-10
hsa05219:Bladder cancer	Small, Medium	15	1.51E-12	1.75E-09
GO:0010604~positive regulation of macromolecule metabolic process	Small, Medium	42	1.77E-12	3.14E-09
GO:0040012~regulation of locomotion	Small, Medium	21	2.25E-12	3.98E-09
GO:0016477~cell migration	Small, Medium	24	5.05E-12	8.94E-09
GO:0040017~positive regulation of locomotion	Small, Medium	16	5.30E-12	9.39E-09
GO:0048514~blood vessel morphogenesis	Small, Medium	21	1.30E-11	2.30E-08
GO:0004713~protein tyrosine kinase activity	Small, Medium	19	1.41E-11	2.05E-08
GO:0030335~positive regulation of cell migration	Small, Medium	15	1.89E-11	3.35E-08
GO:0030334~regulation of cell migration	Small, Medium	19	2.05E-11	3.64E-08
GO:0051674~localization of cell	Small, Medium	24	4.45E-11	7.88E-08
GO:0048870~cell motility	Small, Medium	24	4.45E-11	7.88E-08
GO:0051272~positive regulation of cell motion	Small, Medium	15	7.26E-11	1.29E-07
GO:0008629~induction of apoptosis by intracellular signals	Small, Medium	12	1.59E-10	2.81E-07
GO:0044459~plasma membrane part	Small, Medium	67	2.09E-10	2.81E-07

Supplementary Table 4

Nuclear ITH accompanies genetic ITH across cancers. Spearman rank correlation coefficients between intra-tumoral nuclear diversity and clone number predicted by PyClone (left) and EXPANDS (center) displayed for each cancer type. Positive association between nuclear and genetic ITH persists after taking into account the dependency of both ITH measures on tumor purity (right), suggesting that the observation cannot be explained by a common influence of tumor purity on these ITH measures (see also **Fig. 4** and **Supplementary Figure 7).** Unadjusted p-values are shown.

	PyClone		EXPANDS		EXPANDS (purity normalized)	
	Spearman correlation coefficient	**P-value**	**Spearman correlation coefficient**	**P-value**	**Spearman correlation coefficient**	**P-value**
All cancers	0.012	0.712	0.243	6.27E-14	0.224	4.90E-12
Stomach	0.101	0.331	0.406	4.56E-05	0.381	1.40E-04
Kidney	0.173	0.202	0.413	0.001	0.385	0.002
Head and Neck	0.261	0.005	0.278	0.003	0.266	0.004
Bladder	0.032	0.738	0.246	0.009	0.249	0.008
Glioblastoma	0.150	0.192	0.247	0.029	0.149	0.192
Melanoma	0.158	0.264	0.219	0.115	0.215	0.122
Low-grade glioma	0.236	0.015	0.125	0.168	0.098	0.279
Prostate	0.067	0.626	-0.081	0.538	-0.087	0.509
Thyroid	-0.171	0.255	-0.055	0.676	0.073	0.581
Cervical	0.226	0.205	-0.075	0.680	0.033	0.857
Lung (squam)	-0.362	0.002	-0.042	0.734	-0.069	0.574
Lung (adeno)	-0.107	0.373	0.029	0.813	0.036	0.764

Supplementary Table 5

Definition of covariates used during univariate Cox analysis. MAD := median absolute deviation.

	Covariate	Description
1	amplification abundance	Fraction of tumor metagenome affected by gains or amplifications (deviation from diploid >= +0.25)
2	cnv abundance	Fraction of tumor metagenome affected by CNVs (absolute deviation from diploid >= 0.25)
3	deletion abundance	Fraction of tumor metagenome affected by single copy losses (deviation from diploid <= -0.25)
4	extreme CNV abundance	log |CNV abundance - mean CNV abundance|
5	extreme SNV abundance	|SNV abundance - mean SNV abundance|
6	progression Index	Minimum clone size associated with observed CAN-gene mutations, substracted from 1
7	snv abundance	Count of somatic SNVs
8	Clone number	Number of clones (predicted by EXPANDS or PyClone)
9	Purity normalized clone number	Number of clones normalized to take into account tumor purity
10	Nuclear diversity rank	Histopathological intra-tumor diversity measured as MAD of nuclear intensity and size
11	MKI67 expression	Proliferation rate as measured by KI67 mRNA expression

Supplementary Table 6

Prognostic significance of genomic instability measures across cancers. P-values and hazard ratios from univariate Cox models. P-values below 0.05 are marked blue. The magnitude of the hazard ratio is color-coded (yellow: favorable outcome; red: poor outcome; gray: moderate effect). Where variables did not satisfy the proportionality assumption for the Cox model ($P<0.05$), the corresponding hazard ratios are flagged (*). Two clinical endpoints are shown: **(a)** overall survival and **(b)** progression-free survival.

a

		low/high SNV abundance	low/high CNV abundance	SNV abundance	CNV abundance	deletion abundance	amplification abundance
All cancers (including PRAD & THCA)	p-value (Cox)	0.07	4.79E-08	0.99	0.10	0.59	0.26
	corrected p-value (Cox)	0.34	6.71E-07	0.99	0.45	0.82	0.53
	hazard ratio (Cox)	0.03	0.15	1.01	1.34	1.10	1.20
	# samples	1157	1157	1157	1157	1157	1157
STAD	p-value (Cox)	0.53	0.11	0.42	0.23	0.22	0.01
	corrected p-value (Cox)	0.69	0.22	0.67	0.51	0.65	0.11
	hazard ratio (Cox)	0.21	0.29	0.14	1.99	0.56	3.44
	# samples	142	142	142	142	142	142
GBM	p-value (Cox)	0.39	0.56	0.06	0.59	0.48	0.93
	corrected p-value (Cox)	0.69	0.56	0.38	0.70	0.78	0.93
	hazard ratio (Cox)	0.35	1.66	4.94	0.80	0.71	1.04
	# samples	103	103	103	103	103	103
LGG	p-value (Cox)	1.33E-04	0.07	0.10	0.08	0.50	0.17
	corrected p-value (Cox)	9.33E-04	0.22	0.38	0.45	0.78	0.49
	hazard ratio (Cox)	0.00	0.22	8.22	2.23	1.52	1.87
	# samples	166	166	166	166	166	166
Glioma (GBM+LGG)	p-value (Cox)	2.83E-14	1.36E-03	4.98E-08	0.04	0.38	0.14
	corrected p-value (Cox)	3.96E-13	0.01	6.97E-07	0.45	0.78	0.49
	hazard ratio (Cox)	0.00	0.15	14.85	1.78	1.37	1.51
	# samples	269	269	269	269	269	269
KIRC	p-value (Cox)	0.94	0.16	0.22	0.46	0.23	0.76
	corrected p-value (Cox)	0.94	0.27	0.62	0.65	0.65	0.82
	hazard ratio (Cox)	0.89 *	45.03	3.32	0.60	0.20	1.24
	# samples	65	65	65	65	65	65
HNSC	p-value (Cox)	0.40	0.44	0.62	0.22	0.50	0.64
	corrected p-value (Cox)	0.69	0.56	0.67	0.51	0.78	0.82
	hazard ratio (Cox)	0.52	0.68	0.73	1.74	1.30	1.20
	# samples	165	165	165	165	165	165
LUAD	p-value (Cox)	0.37	0.37	0.30	0.29	0.07	0.63
	corrected p-value (Cox)	0.69	0.56	0.67	0.51	0.49	0.82
	hazard ratio (Cox)	0.23	0.41	0.24	2.29	3.90	0.69
	# samples	77	77	77	77	77	77
BLCA	p-value (Cox)	0.21	0.08	0.11	0.37	0.75	0.21
	corrected p-value (Cox)	0.69	0.22	0.38	0.57	0.86	0.49
	hazard ratio (Cox)	0.14	0.14	0.09	0.59	1.19	0.51
	# samples	114	114	114	114	114	114
LUSC	p-value (Cox)	0.64	0.01	0.60	0.29	0.11	0.68
	corrected p-value (Cox)	0.69	0.05	0.67	0.51	0.52	0.82
	hazard ratio (Cox)	0.32	0.11	0.29	0.45	0.26	1.34
	# samples	85	85	85	85	85	85
SKCM	p-value (Cox)	0.61	0.52	0.62	0.99	0.04	0.16
	corrected p-value (Cox)	0.69	0.56	0.67	0.99	0.49	0.49
	hazard ratio (Cox)	0.49	0.46	0.51	1.01	5.76	0.36
	# samples	54	54	54	54	54	54
CESC	p-value (Cox)	0.56	0.11	0.44	0.28	0.86	0.11
	corrected p-value (Cox)	0.69	0.22	0.67	0.51	0.86	0.49
	hazard ratio (Cox)	0.14	0.13	0.01	3.30	0.78	5.33
	# samples	33	33	33	33	33	33

36

		low/high SNV abundance	low/high CNV abundance	SNV abundance	CNV abundance	deletion abundance	amplification abundance
All cancers (including PRAD & THCA)	p-value (Cox)	0.02	1.62E-06	0.27	0.25	1.00	0.27
	corrected p-value (Cox)	0.07	2.27E-05	0.63	0.73	1.00	0.53
	hazard ratio (Cox)	0.02	0.21	0.33	1.19	1.00	1.17
	# samples	1157	1157	1157	1157	1157	1157
STAD	p-value (Cox)	0.31	0.30	0.20	0.71	0.15	0.04
	corrected p-value (Cox)	0.66	0.53	0.57	0.86	0.89	0.53
	hazard ratio (Cox)	0.06	0.48	0.04 *	1.19	0.55	2.34
	# samples	142	142	142	142	142	142
GBM	p-value (Cox)	0.37	0.47	4.38E-03	0.85	0.57	0.47
	corrected p-value (Cox)	0.66	0.68	0.02	0.86	0.92	0.60
	hazard ratio (Cox)	0.38	1.73	11.26	1.07	0.77	1.32
	# samples	103	103	103	103	103	103
LGG	p-value (Cox)	0.01	0.16	3.48E-05	0.27	0.68	0.39
	corrected p-value (Cox)	0.06	0.31	2.44E-04	0.73	0.92	0.60
	hazard ratio (Cox)	0.01	0.36	29.14	1.49	1.22	1.37
	# samples	166	166	166	166	166	166
Glioma (GBM+LGG)	p-value (Cox)	4.44E-15	4.84E-04	5.55E-16	0.05	0.38	0.16
	corrected p-value (Cox)	6.22E-14	3.39E-03	7.77E-15	0.64	0.89	0.53
	hazard ratio (Cox)	0.00	0.16	38.52 *	1.62	1.31	1.41
	# samples	269	269	269	269	269	269
KIRC	p-value (Cox)	0.74	0.15	0.43	0.86	0.28	0.24
	corrected p-value (Cox)	0.74	0.31	0.63	0.86	0.89	0.53
	hazard ratio (Cox)	0.60 *	23.23	2.15	1.10	0.33	2.01
	# samples	65	65	65	65	65	65
HNSC	p-value (Cox)	0.15	0.76	0.32	0.11	0.69	0.23
	corrected p-value (Cox)	0.42	0.76	0.63	0.73	0.92	0.53
	hazard ratio (Cox)	0.34	0.87	0.55	1.92	1.16	1.52
	# samples	165	165	165	165	165	165
LUAD	p-value (Cox)	0.59	0.61	0.64	0.31	0.33	0.94
	corrected p-value (Cox)	0.66	0.68	0.70	0.73	0.89	0.94
	hazard ratio (Cox)	0.51	0.67	0.62	1.87	1.82	1.05
	# samples	77	77	77	77	77	77
BLCA	p-value (Cox)	0.13	0.07	0.07	0.72	0.76	0.43
	corrected p-value (Cox)	0.42	0.26	0.25	0.86	0.92	0.60
	hazard ratio (Cox)	0.09	0.15	0.07	0.81	1.17	0.68
	# samples	114	114	114	114	114	114
LUSC	p-value (Cox)	0.62	0.02	0.65	0.52	0.34	0.82
	corrected p-value (Cox)	0.66	0.09	0.70	0.86	0.89	0.88
	hazard ratio (Cox)	0.34	0.16	0.41	0.64	0.52	1.16
	# samples	85	85	85	85	85	85
SKCM	p-value (Cox)	0.53	0.63	0.45	0.81	0.07	0.29
	corrected p-value (Cox)	0.66	0.68	0.63	0.86	0.89	0.53
	hazard ratio (Cox)	0.41	0.56	0.35	1.24	4.44	0.48
	# samples	54	54	54	54	54	54
CESC	p-value (Cox)	0.56	0.11	0.44	0.28	0.86	0.11
	corrected p-value (Cox)	0.66	0.30	0.63	0.73	0.92	0.53
	hazard ratio (Cox)	0.14	0.13	0.01	3.30	0.78	5.33
	# samples	33	33	33	33	33	33

Supplementary Table 7
Clinical annotation of analyzed TCGA samples. Cancer type, overall survival and progression free survival are shown for individuals across 12 cancer types. Of the 1,165 individuals, 8 (0.7%) had missing overall and progression-free survival, without any follow-up time available. A value of 1 in column "censored" indicates that the corresponding entry in the prior column is censored. Pathologic stage and administration of adjuvant chemo- and radiation therapy are indicated. NA := not available.

TCGA patient barcode	cancer type	days to death	censored	days to progression	censored	stage	chemo-therapy	radiation-therapy
TCGA-EL-A3CT	THCA	1825	1	1825	1	4	0	0
TCGA-EL-A3CU	THCA	1825	1	1825	1	1	0	1
TCGA-EL-A3GR	THCA	1825	1	1825	1	2	0	1
TCGA-EL-A3GY	THCA	1825	1	1825	1	2	0	1
TCGA-EL-A3H5	THCA	1825	1	1825	1	4	0	1
TCGA-EL-A3GQ	THCA	1528	1	1528	1	1	0	0
TCGA-BJ-A192	THCA	1349	1	1349	1	2	0	0
TCGA-EL-A3CV	THCA	1154	1	1154	1	3	0	1
TCGA-DJ-A3V0	THCA	1125	1	1125	1	4	0	1
TCGA-DJ-A2Q0	THCA	1045	1	1045	1	1	0	0
TCGA-EL-A3CL	THCA	963	0	963	0	1	0	0
TCGA-DJ-A3VM	THCA	840	1	840	1	1	0	1
TCGA-DJ-A3V6	THCA	818	1	818	1	2	0	1
TCGA-EM-A1CS	THCA	817	1	817	1	1	0	0
TCGA-BJ-A0YZ	THCA	754	1	754	1	1	0	0
TCGA-EL-A4KG	THCA	739	1	739	1	1	0	0
TCGA-EL-A4KI	THCA	727	1	727	1	2	0	1
TCGA-BJ-A4O9	THCA	714	1	714	1	1	0	0
TCGA-DJ-A3V7	THCA	706	1	706	1	2	0	1
TCGA-DJ-A3VB	THCA	697	1	697	1	3	0	1
TCGA-DO-A1K0	THCA	655	1	655	1	3	0	1
TCGA-DJ-A3VD	THCA	639	1	639	1	1	0	1
TCGA-DJ-A3V9	THCA	623	1	623	1	2	0	1
TCGA-EM-A1YB	THCA	592	1	592	1	1	0	1
TCGA-DJ-A4UQ	THCA	580	1	580	1	3	0	1
TCGA-DJ-A3VE	THCA	577	1	577	1	1	0	0
TCGA-BJ-A3PU	THCA	567	1	567	1	3	0	1
TCGA-BJ-A0Z2	THCA	554	1	554	1	2	0	1
TCGA-DJ-A4UL	THCA	554	1	554	1	1	0	0
TCGA-EM-A1CT	THCA	553	1	553	1	1	0	1
TCGA-EM-A2P2	THCA	526	1	526	1	2	0	1
TCGA-DJ-A3VL	THCA	524	1	524	1	1	0	0
TCGA-BJ-A0ZE	THCA	509	1	509	1	2	0	0
TCGA-BJ-A3EZ	THCA	487	1	487	1	3	0	1
TCGA-DE-A0Y2	THCA	469	1	469	1	2	0	0
TCGA-DJ-A4UR	THCA	469	1	469	1	4	0	1
TCGA-DJ-A4UW	THCA	447	1	447	1	1	0	1
TCGA-EM-A3O3	THCA	441	1	441	1	2	0	1
TCGA-E8-A417	THCA	434	1	434	1	2	0	0
TCGA-E3-A3E5	THCA	427	1	427	1	4	0	1
TCGA-BJ-A0Z0	THCA	419	1	419	1	1	0	0
TCGA-DJ-A2QA	THCA	378	1	378	1	2	0	0
TCGA-E3-A3DZ	THCA	367	1	367	1	2	0	1
TCGA-EM-A2CM	THCA	357	1	357	1	2	0	1
TCGA-DE-A4MB	THCA	352	1	352	1	3	0	1
TCGA-DJ-A13M	THCA	287	1	287	1	1	0	0
TCGA-EM-A3AP	THCA	254	1	254	1	1	0	0
TCGA-DJ-A3VG	THCA	253	1	253	1	1	0	0
TCGA-BJ-A0Z9	THCA	251	1	251	1	2	0	1
TCGA-DJ-A2PO	THCA	243	1	243	1	1	0	0
TCGA-E8-A437	THCA	234	1	234	1	NA	0	0
TCGA-DJ-A1QL	THCA	219	1	219	1	1	0	0
TCGA-DJ-A1QG	THCA	212	1	212	1	1	0	0
TCGA-DJ-A2PP	THCA	162	1	162	1	1	0	0
TCGA-BJ-A28V	THCA	155	1	155	1	2	0	0
TCGA-BJ-A0ZB	THCA	122	1	122	1	3	0	0
TCGA-DJ-A13R	THCA	92	1	92	1	2	0	0
TCGA-E8-A418	THCA	92	1	92	1	3	0	0

38

TCGA-BJ-A28Z	THCA	37	1	37	1	3	0	0
TCGA-CE-A484	THCA	12	1	12	1	2	0	0
TCGA-HF-7131	STAD	NA	NA	NA	NA	1	0	1
TCGA-HF-7132	STAD	NA	NA	NA	NA	2	1	1
TCGA-HF-7133	STAD	NA	NA	NA	NA	4	1	1
TCGA-HF-7134	STAD	NA	NA	NA	NA	1	0	0
TCGA-CG-4438	STAD	1645	1	1645	1	4	0	0
TCGA-CG-4444	STAD	1431	1	1431	1	3	1	1
TCGA-CG-5718	STAD	1095	0	1095	0	2	0	0
TCGA-BR-7704	STAD	1072	1	1072	1	2	0	0
TCGA-BR-6852	STAD	1002	1	1002	1	2	0	0
TCGA-BR-6566	STAD	997	1	997	1	2	0	0
TCGA-CG-4477	STAD	942	1	365	0	1	1	1
TCGA-BR-6802	STAD	940	1	807	0	4	0	0
TCGA-CG-4443	STAD	912	1	912	1	1	0	0
TCGA-HU-A4GN	STAD	912	1	912	1	2	1	0
TCGA-BR-7716	STAD	852	1	852	1	3	0	0
TCGA-HU-A4HD	STAD	834	1	834	1	4	0	0
TCGA-CG-4304	STAD	822	1	822	1	1	0	0
TCGA-HJ-7597	STAD	805	0	795	0	1	1	1
TCGA-HU-A4GF	STAD	785	1	785	1	2	0	0
TCGA-BR-6705	STAD	779	0	779	0	4	0	0
TCGA-BR-8484	STAD	766	0	766	0	4	0	0
TCGA-BR-7703	STAD	753	1	753	1	1	0	0
TCGA-HU-A4G2	STAD	739	1	739	1	3	1	0
TCGA-HU-A4G9	STAD	736	1	736	1	1	0	0
TCGA-BR-7707	STAD	728	1	728	1	1	0	0
TCGA-CG-4475	STAD	699	1	699	1	3	0	0
TCGA-HU-A4GD	STAD	692	1	692	1	3	1	0
TCGA-FP-7998	STAD	678	1	678	1	4	1	0
TCGA-BR-A4CQ	STAD	677	1	677	1	4	0	0
TCGA-BR-6801	STAD	642	1	642	1	2	0	0
TCGA-BR-A4PD	STAD	628	1	628	1	3	0	0
TCGA-BR-8081	STAD	625	1	625	1	3	0	0
TCGA-BR-A4PE	STAD	621	1	621	1	1	0	0
TCGA-BR-8486	STAD	615	1	615	1	1	0	0
TCGA-CG-4300	STAD	609	0	609	0	4	0	0
TCGA-BR-6707	STAD	605	0	426	0	2	1	0
TCGA-MX-A5UJ	STAD	600	1	600	1	4	0	0
TCGA-FP-7829	STAD	594	1	594	1	3	1	1
TCGA-BR-8361	STAD	593	1	593	1	4	0	0
TCGA-HU-A4H3	STAD	589	1	589	1	4	1	1
TCGA-CG-4449	STAD	580	1	336	0	2	0	0
TCGA-CG-4466	STAD	577	1	577	1	1	0	0
TCGA-D7-6520	STAD	573	1	46	0	3	0	1
TCGA-BR-7959	STAD	569	1	569	1	4	1	0
TCGA-D7-6521	STAD	564	1	192	0	3	1	0
TCGA-BR-7717	STAD	552	0	552	0	4	0	0
TCGA-BR-6706	STAD	549	0	402	0	3	1	0
TCGA-D7-A4YU	STAD	500	1	500	1	4	1	0
TCGA-EQ-A4SO	STAD	494	1	494	1	4	1	1
TCGA-D7-6815	STAD	486	1	486	1	3	0	0
TCGA-BR-8589	STAD	481	1	481	1	4	0	0
TCGA-BR-8680	STAD	481	1	481	1	4	1	0
TCGA-BR-8296	STAD	474	0	390	0	4	0	0
TCGA-BR-7722	STAD	466	0	466	0	3	0	0
TCGA-D7-6528	STAD	463	1	463	1	1	0	0
TCGA-D7-A4YX	STAD	461	1	461	1	3	0	0
TCGA-BR-8373	STAD	450	1	450	1	4	1	0
TCGA-D7-A4Z0	STAD	449	1	449	1	2	0	1
TCGA-D7-8576	STAD	446	0	204	0	4	0	1
TCGA-F1-6874	STAD	440	1	440	1	1	0	0
TCGA-BR-A4J2	STAD	431	1	431	1	3	1	0
TCGA-FP-7916	STAD	428	0	428	0	4	1	0
TCGA-BR-8369	STAD	427	1	419	0	4	0	1
TCGA-BR-A44U	STAD	422	0	422	0	4	0	0
TCGA-D7-A4YY	STAD	419	1	419	1	4	0	1
TCGA-BR-A4J8	STAD	411	1	411	1	4	1	0
TCGA-D7-6525	STAD	406	0	171	0	3	1	0
TCGA-CD-5801	STAD	401	0	401	0	3	0	0

TCGA-BR-8362	STAD	398	0	356	0	4	0	0
TCGA-BR-8286	STAD	394	1	394	1	2	0	0
TCGA-HU-A4H2	STAD	394	1	394	1	4	0	0
TCGA-BR-A4IY	STAD	392	1	392	1	3	1	0
TCGA-BR-7196	STAD	390	1	348	0	4	1	0
TCGA-BR-8588	STAD	389	1	389	1	3	0	0
TCGA-D7-6817	STAD	389	1	389	1	4	0	1
TCGA-D7-5578	STAD	385	1	385	1	4	0	0
TCGA-CD-A4MJ	STAD	384	1	69	0	1	0	1
TCGA-BR-7851	STAD	378	1	378	1	3	0	0
TCGA-CD-A48A	STAD	378	1	378	1	2	0	1
TCGA-D7-5577	STAD	376	1	376	0	4	0	0
TCGA-BR-8078	STAD	373	1	373	1	3	0	0
TCGA-CD-A4MH	STAD	371	1	371	1	2	0	1
TCGA-BR-6709	STAD	370	0	370	0	4	1	0
TCGA-HU-8604	STAD	368	1	368	1	2	1	0
TCGA-CG-4455	STAD	366	1	366	1	2	0	0
TCGA-D7-5579	STAD	363	1	363	1	4	0	0
TCGA-BR-A4QL	STAD	352	1	352	1	4	0	0
TCGA-BR-8678	STAD	351	1	351	1	1	0	0
TCGA-BR-8060	STAD	348	0	348	0	3	0	0
TCGA-HU-8602	STAD	347	1	347	1	3	1	0
TCGA-CD-A489	STAD	344	0	277	0	2	0	0
TCGA-D7-6820	STAD	344	1	344	1	2	0	0
TCGA-BR-8690	STAD	325	1	325	1	4	1	0
TCGA-HU-8608	STAD	323	1	323	1	4	1	0
TCGA-D7-6818	STAD	321	1	278	0	4	0	1
TCGA-HU-A4GX	STAD	310	1	310	1	4	1	0
TCGA-BR-8683	STAD	300	0	300	0	4	0	0
TCGA-HU-A4H6	STAD	294	1	294	1	4	1	0
TCGA-BR-8590	STAD	284	0	223	0	4	0	0
TCGA-CD-A487	STAD	284	1	284	1	3	0	0
TCGA-BR-7197	STAD	280	1	280	1	2	0	0
TCGA-BR-6565	STAD	279	0	279	0	3	0	0
TCGA-CG-4465	STAD	274	0	274	0	4	1	0
TCGA-HU-A4GP	STAD	273	1	273	1	2	1	0
TCGA-HU-A4H8	STAD	270	1	270	1	1	1	0
TCGA-BR-8687	STAD	250	0	250	0	4	0	0
TCGA-BR-8284	STAD	245	0	245	0	4	0	0
TCGA-CG-4437	STAD	245	1	245	1	2	0	0
TCGA-CG-4436	STAD	243	1	243	1	1	0	0
TCGA-BR-8297	STAD	225	1	225	1	4	0	0
TCGA-CG-4469	STAD	215	0	215	0	4	1	0
TCGA-CG-5717	STAD	212	0	120	0	2	1	0
TCGA-CD-A4MG	STAD	200	0	74	0	2	0	0
TCGA-F1-6177	STAD	200	1	200	1	1	0	0
TCGA-HU-A4GT	STAD	198	1	198	1	2	1	0
TCGA-BR-8360	STAD	188	1	188	1	2	0	0
TCGA-HU-A4G3	STAD	170	1	170	1	3	1	0
TCGA-FP-A4BF	STAD	168	0	159	0	4	0	0
TCGA-BR-8483	STAD	164	1	164	1	4	0	0
TCGA-CG-4440	STAD	122	0	122	0	4	0	0
TCGA-BR-7901	STAD	105	0	91	0	3	0	0
TCGA-CD-A486	STAD	104	1	104	1	2	0	0
TCGA-IN-8663	STAD	103	0	103	0	3	0	0
TCGA-CD-5799	STAD	99	1	99	1	2	0	0
TCGA-CG-4301	STAD	92	1	92	1	4	0	0
TCGA-BR-8289	STAD	81	0	81	0	4	0	0
TCGA-IP-7968	STAD	77	1	77	1	4	0	0
TCGA-BR-A4CS	STAD	45	0	45	0	4	0	0
TCGA-BR-A4PF	STAD	35	1	35	1	4	0	0
TCGA-CG-5719	STAD	31	1	31	1	4	0	0
TCGA-BR-A4J1	STAD	22	0	22	0	4	0	0
TCGA-BR-8077	STAD	21	1	21	1	4	0	0
TCGA-BR-A4J6	STAD	20	1	20	1	2	0	0
TCGA-BR-8285	STAD	17	0	17	0	4	0	0
TCGA-BR-A4J4	STAD	16	1	16	1	4	0	0
TCGA-BR-8677	STAD	15	1	15	1	4	0	0
TCGA-CD-5802	STAD	9	1	9	1	2	0	0
TCGA-BR-8363	STAD	8	0	8	0	4	0	0

40

TCGA-BR-8381	STAD	8	1	8	1	3	1	0
TCGA-CD-8533	STAD	4	1	4	1	2	0	0
TCGA-CD-A4MI	STAD	3	1	3	1	3	0	0
TCGA-HU-A4GQ	STAD	3	0	3	0	4	0	0
TCGA-BR-A4CR	STAD	0	1	0	1	4	0	0
TCGA-CG-4442	STAD	0	1	0	1	1	0	0
TCGA-CG-4462	STAD	0	0	0	0	4	0	0
TCGA-CG-4476	STAD	0	1	0	1	4	0	0
TCGA-HR-A2OH	SKCM	1825	1	1825	1	4	1	1
TCGA-BF-A1Q0	SKCM	831	1	831	1	3	0	0
TCGA-GN-A26C	SKCM	821	0	821	0	4	0	1
TCGA-EB-A4XL	SKCM	777	1	777	1	3	0	0
TCGA-FS-A1ZN	SKCM	730	0	730	0	4	0	0
TCGA-FR-A3R1	SKCM	685	1	685	1	3	0	0
TCGA-EB-A3XC	SKCM	650	1	650	1	3	0	0
TCGA-EB-A24D	SKCM	645	1	645	1	4	1	0
TCGA-FW-A5DX	SKCM	640	1	640	1	NA	0	1
TCGA-EB-A24C	SKCM	632	1	465	0	3	1	0
TCGA-EB-A1NK	SKCM	613	1	613	1	3	0	0
TCGA-EB-A4OY	SKCM	593	1	593	1	4	0	0
TCGA-EB-A551	SKCM	590	1	590	1	4	0	0
TCGA-EB-A431	SKCM	568	1	568	1	3	0	0
TCGA-D9-A4Z6	SKCM	561	0	561	0	3	0	0
TCGA-D9-A1X3	SKCM	551	1	551	1	4	0	1
TCGA-EB-A51B	SKCM	537	1	537	1	3	0	0
TCGA-IH-A3EA	SKCM	524	1	524	1	3	0	0
TCGA-D9-A3Z4	SKCM	519	0	519	0	4	0	0
TCGA-ER-A19K	SKCM	469	0	469	0	3	1	0
TCGA-EB-A6R0	SKCM	467	1	467	1	3	0	0
TCGA-GN-A263	SKCM	467	0	467	0	4	0	0
TCGA-EB-A5FP	SKCM	454	0	454	0	4	1	0
TCGA-EB-A42Z	SKCM	441	1	441	1	4	0	0
TCGA-EB-A42Y	SKCM	440	1	440	1	3	0	0
TCGA-EB-A3XD	SKCM	430	1	430	1	3	0	0
TCGA-EB-A5UM	SKCM	414	1	414	1	3	0	0
TCGA-EB-A3XB	SKCM	408	1	408	1	3	0	0
TCGA-EB-A5SE	SKCM	401	0	401	0	2	0	0
TCGA-EB-A57M	SKCM	399	1	399	1	4	1	0
TCGA-EB-A6QY	SKCM	382	1	382	1	3	0	0
TCGA-EB-A299	SKCM	378	1	378	1	1	0	0
TCGA-EB-A5SF	SKCM	369	0	369	0	3	0	0
TCGA-FR-A2OS	SKCM	368	0	368	0	3	1	0
TCGA-EB-A6QZ	SKCM	352	0	352	0	2	0	1
TCGA-EB-A3Y7	SKCM	326	0	326	0	4	0	0
TCGA-EB-A4P0	SKCM	326	0	326	0	3	0	0
TCGA-EB-A41B	SKCM	291	1	291	1	3	0	0
TCGA-EB-A3XF	SKCM	278	1	278	1	3	0	0
TCGA-EB-A550	SKCM	264	0	264	0	3	0	0
TCGA-EB-A41A	SKCM	262	1	262	1	3	0	0
TCGA-EB-A553	SKCM	226	1	226	1	3	1	0
TCGA-D9-A4Z5	SKCM	218	1	218	1	3	0	1
TCGA-D9-A4Z2	SKCM	190	0	190	0	4	0	0
TCGA-EB-A3XE	SKCM	180	1	180	1	2	0	0
TCGA-GN-A269	SKCM	170	0	170	0	4	0	0
TCGA-EB-A3Y6	SKCM	126	1	126	1	3	1	0
TCGA-EB-A44O	SKCM	81	1	81	1	3	0	0
TCGA-GF-A2C7	SKCM	21	1	21	1	3	0	0
TCGA-BF-A1PV	SKCM	14	1	14	1	3	0	0
TCGA-BF-A3DM	SKCM	14	1	14	1	3	0	0
TCGA-HR-A2OG	SKCM	7	1	7	1	NA	0	0
TCGA-EB-A430	SKCM	2	1	2	1	3	0	0
TCGA-EB-A4IS	SKCM	0	1	0	1	2	0	0
TCGA-EJ-5519	PRAD	1825	1	1825	1	3	0	0
TCGA-EJ-7115	PRAD	1825	1	1825	1	2	0	0
TCGA-EJ-7123	PRAD	1825	1	1825	1	1	0	0
TCGA-G9-6332	PRAD	1825	1	1180	0	2	0	0
TCGA-G9-6333	PRAD	1825	1	1825	1	1	0	0
TCGA-HC-7078	PRAD	1825	1	1825	1	2	0	0
TCGA-HI-7168	PRAD	1825	1	1825	1	2	0	1
TCGA-HI-7169	PRAD	1825	1	1825	1	2	0	0

41

TCGA-HI-7170	PRAD	1825	1	1825	1	1	0	0
TCGA-G9-6494	PRAD	1771	1	1771	1	3	0	0
TCGA-EJ-5518	PRAD	1590	1	1590	1	3	0	0
TCGA-EJ-5511	PRAD	1476	1	1476	1	2	0	0
TCGA-EJ-5509	PRAD	1464	1	1464	1	1	0	0
TCGA-EJ-5517	PRAD	1454	1	1454	1	1	0	0
TCGA-G9-6362	PRAD	1443	1	1443	1	2	0	0
TCGA-EJ-5516	PRAD	1416	1	1416	1	2	0	0
TCGA-G9-6361	PRAD	1415	1	1415	1	2	0	0
TCGA-G9-6363	PRAD	1378	1	1378	1	3	0	0
TCGA-EJ-5501	PRAD	1365	1	1365	1	2	0	0
TCGA-HI-7171	PRAD	1329	0	1329	0	2	0	1
TCGA-EJ-5524	PRAD	1310	1	265	0	2	0	1
TCGA-G9-6329	PRAD	1266	1	1266	1	1	0	0
TCGA-HC-7213	PRAD	1219	1	170	0	2	0	1
TCGA-G9-6369	PRAD	1215	1	1215	1	1	0	0
TCGA-EJ-5527	PRAD	1209	1	1209	1	2	0	0
TCGA-G9-6364	PRAD	1198	1	1198	1	2	0	0
TCGA-EJ-5508	PRAD	1184	1	1184	1	2	0	0
TCGA-EJ-5526	PRAD	1179	1	537	0	3	0	0
TCGA-EJ-7782	PRAD	1167	1	1167	1	1	0	0
TCGA-EJ-7314	PRAD	1150	1	1150	1	2	0	0
TCGA-EJ-5510	PRAD	1116	1	1116	1	1	0	0
TCGA-EJ-5525	PRAD	1115	1	546	0	1	0	0
TCGA-HC-7080	PRAD	1106	1	894	0	1	0	0
TCGA-EJ-5514	PRAD	1102	1	1102	1	1	0	0
TCGA-CH-5751	PRAD	1065	1	365	0	4	0	0
TCGA-EJ-7315	PRAD	1008	1	1008	1	2	0	0
TCGA-G9-7525	PRAD	994	1	994	1	1	0	0
TCGA-HC-7821	PRAD	956	1	956	1	3	0	1
TCGA-CH-5752	PRAD	943	1	943	1	2	0	1
TCGA-G9-7521	PRAD	942	1	942	1	3	0	0
TCGA-EJ-5505	PRAD	922	1	922	1	1	0	0
TCGA-EJ-5542	PRAD	884	1	884	1	2	0	0
TCGA-CH-5794	PRAD	882	1	882	1	1	0	0
TCGA-EJ-5504	PRAD	880	1	880	1	3	0	0
TCGA-HC-7212	PRAD	870	1	870	1	1	0	1
TCGA-FC-7708	PRAD	864	1	864	1	2	0	0
TCGA-G9-7523	PRAD	857	1	857	1	2	0	0
TCGA-EJ-5506	PRAD	827	1	827	1	3	0	0
TCGA-EJ-5494	PRAD	826	1	826	1	2	0	0
TCGA-EJ-7321	PRAD	824	1	824	1	2	0	0
TCGA-G9-6373	PRAD	811	1	811	1	2	0	0
TCGA-EJ-7783	PRAD	787	1	787	1	2	0	0
TCGA-HC-7752	PRAD	782	1	782	1	1	0	0
TCGA-EJ-7784	PRAD	781	1	781	1	1	0	0
TCGA-EJ-7317	PRAD	771	1	771	1	1	0	0
TCGA-EJ-7331	PRAD	742	1	742	1	1	0	0
TCGA-EJ-5507	PRAD	727	1	727	1	3	0	0
TCGA-EJ-7781	PRAD	727	1	727	1	1	0	0
TCGA-HC-7740	PRAD	717	1	717	1	1	0	0
TCGA-HC-8216	PRAD	682	1	682	1	NA	0	0
TCGA-CH-5739	PRAD	671	1	671	1	2	0	0
TCGA-EJ-7785	PRAD	625	1	625	1	2	0	0
TCGA-J4-8198	PRAD	614	1	614	1	2	0	0
TCGA-EJ-7797	PRAD	606	1	606	1	1	0	0
TCGA-HC-7075	PRAD	601	1	601	1	1	0	0
TCGA-EJ-5496	PRAD	595	1	595	1	1	0	0
TCGA-EJ-7789	PRAD	552	1	552	1	2	0	0
TCGA-EJ-7792	PRAD	526	1	526	1	1	0	0
TCGA-HC-8265	PRAD	483	1	483	1	2	0	1
TCGA-HC-7209	PRAD	440	1	440	1	1	0	0
TCGA-EJ-7788	PRAD	430	1	430	1	2	0	0
TCGA-CH-5743	PRAD	425	1	425	0	1	0	0
TCGA-EJ-5497	PRAD	405	1	405	1	1	0	0
TCGA-CH-5750	PRAD	396	1	396	1	1	0	0
TCGA-CH-5741	PRAD	395	1	395	1	3	0	1
TCGA-J4-8200	PRAD	374	1	374	1	NA	0	0
TCGA-CH-5789	PRAD	304	1	304	1	2	0	0
TCGA-EJ-7330	PRAD	191	1	191	1	2	0	0

TCGA-H9-7775	PRAD	185	1	185	1	1	0	0
TCGA-G9-6366	PRAD	101	1	101	1	2	0	0
TCGA-CH-5737	PRAD	91	1	91	1	1	0	0
TCGA-CH-5745	PRAD	91	1	91	1	2	0	0
TCGA-CH-5792	PRAD	91	1	91	1	2	0	0
TCGA-HC-7231	PRAD	72	1	72	1	1	0	0
TCGA-CH-5754	PRAD	62	1	62	1	3	0	0
TCGA-HC-7230	PRAD	51	1	51	1	1	0	0
TCGA-HC-7744	PRAD	51	1	51	1	2	0	0
TCGA-HC-7742	PRAD	45	1	45	1	2	0	0
TCGA-CH-5740	PRAD	31	1	31	1	1	0	0
TCGA-CH-5748	PRAD	31	1	31	1	2	0	0
TCGA-CH-5753	PRAD	31	1	31	1	3	0	0
TCGA-HC-7736	PRAD	22	1	22	1	1	0	0
TCGA-HC-7077	PRAD	0	1	0	1	2	0	0
TCGA-63-7021	LUSC	NA	NA	NA	NA	1	0	0
TCGA-63-7023	LUSC	NA	NA	NA	NA	1	1	1
TCGA-21-1082	LUSC	1825	1	1825	1	1	0	0
TCGA-34-5231	LUSC	1825	1	1825	1	1	0	0
TCGA-34-5232	LUSC	1825	1	1825	1	1	0	0
TCGA-58-8391	LUSC	1825	1	1825	1	3	1	1
TCGA-77-6843	LUSC	1825	1	1825	1	1	0	0
TCGA-77-8130	LUSC	1825	1	1825	1	2	0	0
TCGA-NC-A5HE	LUSC	1825	1	1825	1	2	1	1
TCGA-34-5234	LUSC	1715	1	1715	1	1	0	0
TCGA-77-8133	LUSC	1640	0	1640	0	1	0	0
TCGA-21-5784	LUSC	1268	1	1268	1	1	0	0
TCGA-58-8393	LUSC	1058	1	1058	1	1	0	0
TCGA-21-5786	LUSC	1032	1	817	0	1	0	0
TCGA-85-8354	LUSC	995	1	995	1	1	0	0
TCGA-21-5782	LUSC	962	0	962	0	1	0	0
TCGA-34-5927	LUSC	941	1	218	0	1	0	1
TCGA-58-A46N	LUSC	910	1	630	0	1	0	1
TCGA-43-6647	LUSC	757	1	757	1	2	1	0
TCGA-34-5239	LUSC	707	1	707	1	3	0	0
TCGA-90-A4EE	LUSC	688	1	688	1	2	1	0
TCGA-43-6770	LUSC	653	1	653	1	1	0	0
TCGA-56-A4ZJ	LUSC	640	1	640	1	1	0	0
TCGA-94-7033	LUSC	640	1	640	1	1	1	0
TCGA-56-A49D	LUSC	637	1	637	1	3	0	0
TCGA-90-A4ED	LUSC	615	1	615	1	1	0	0
TCGA-56-A4BW	LUSC	585	1	585	1	2	0	0
TCGA-J1-A4AH	LUSC	581	1	581	1	1	1	0
TCGA-43-5668	LUSC	559	0	470	0	1	1	0
TCGA-56-5898	LUSC	555	1	555	1	1	0	0
TCGA-85-A4QQ	LUSC	553	1	553	1	1	0	0
TCGA-34-5928	LUSC	552	1	552	1	2	0	0
TCGA-56-A4BY	LUSC	543	0	543	0	1	0	1
TCGA-85-A4JB	LUSC	539	1	539	1	2	0	0
TCGA-34-5241	LUSC	515	0	515	0	1	0	0
TCGA-56-8504	LUSC	510	1	510	1	1	0	0
TCGA-85-8351	LUSC	510	1	510	1	2	0	0
TCGA-96-A4JL	LUSC	504	1	504	1	2	1	0
TCGA-85-A50Z	LUSC	493	1	462	0	1	0	0
TCGA-85-A510	LUSC	482	1	363	0	2	0	0
TCGA-56-8629	LUSC	481	1	481	1	1	0	0
TCGA-85-A511	LUSC	455	0	390	0	2	0	0
TCGA-68-A59J	LUSC	448	1	448	1	1	0	0
TCGA-85-8071	LUSC	428	1	428	1	1	0	0
TCGA-46-6026	LUSC	423	1	423	1	2	1	1
TCGA-58-8388	LUSC	412	0	412	0	1	0	0
TCGA-68-8251	LUSC	406	1	406	1	1	1	0
TCGA-56-A4BX	LUSC	405	1	405	1	1	0	0
TCGA-85-6561	LUSC	395	1	395	1	1	1	1
TCGA-77-8131	LUSC	383	0	383	0	1	0	0
TCGA-85-A53L	LUSC	377	1	377	1	1	0	0
TCGA-43-6143	LUSC	376	1	376	1	1	0	0
TCGA-34-5240	LUSC	365	1	365	1	2	1	0
TCGA-43-A474	LUSC	353	1	353	1	1	1	0
TCGA-77-8140	LUSC	351	0	351	0	2	0	0

TCGA-21-5787	LUSC	329	0	103	0	3	0	1
TCGA-46-6025	LUSC	324	1	324	1	2	1	0
TCGA-56-8625	LUSC	315	0	272	0	3	0	0
TCGA-85-8277	LUSC	307	0	307	0	3	0	0
TCGA-43-A475	LUSC	296	1	296	1	2	1	1
TCGA-21-1081	LUSC	284	0	284	0	2	0	1
TCGA-34-5236	LUSC	276	0	113	0	2	0	1
TCGA-37-4130	LUSC	247	1	247	1	1	0	0
TCGA-68-8250	LUSC	244	1	244	1	1	0	0
TCGA-37-4133	LUSC	238	1	238	1	3	0	0
TCGA-37-4132	LUSC	227	1	227	1	2	0	0
TCGA-68-7757	LUSC	211	1	211	1	1	0	0
TCGA-96-8170	LUSC	211	1	211	1	1	0	0
TCGA-37-4135	LUSC	207	1	207	1	1	0	0
TCGA-37-4129	LUSC	200	1	200	1	1	0	0
TCGA-43-6771	LUSC	166	0	154	0	1	0	0
TCGA-92-8063	LUSC	122	1	122	1	3	1	1
TCGA-37-3783	LUSC	120	1	120	1	4	0	0
TCGA-43-6773	LUSC	116	0	116	0	2	0	0
TCGA-37-5819	LUSC	103	1	103	1	3	0	0
TCGA-43-8118	LUSC	89	0	89	0	1	1	0
TCGA-98-8020	LUSC	84	0	84	0	3	0	0
TCGA-92-8065	LUSC	70	1	70	1	2	0	0
TCGA-56-6545	LUSC	62	1	62	1	1	0	0
TCGA-85-8288	LUSC	54	1	54	1	1	0	0
TCGA-56-8624	LUSC	36	1	36	1	2	0	0
TCGA-34-7107	LUSC	34	0	34	0	1	0	0
TCGA-56-6546	LUSC	19	0	19	0	1	0	0
TCGA-37-4141	LUSC	12	1	12	1	1	0	0
TCGA-56-5897	LUSC	3	1	3	1	1	0	0
TCGA-58-8386	LUSC	1	0	1	0	3	0	0
TCGA-46-3769	LUSC	0	1	0	1	3	0	0
TCGA-38-4625	LUAD	1825	1	1825	1	1	0	0
TCGA-38-4626	LUAD	1825	1	1825	1	1	0	0
TCGA-62-8399	LUAD	1825	1	1825	1	3	0	0
TCGA-62-A46U	LUAD	1825	1	1825	1	2	1	0
TCGA-64-5774	LUAD	1825	1	246	0	1	0	1
TCGA-64-1679	LUAD	1686	1	1686	1	2	1	0
TCGA-62-A46S	LUAD	1653	0	1653	0	1	0	0
TCGA-64-5781	LUAD	1559	1	96	0	1	1	0
TCGA-62-8402	LUAD	1498	0	772	0	3	0	1
TCGA-38-4628	LUAD	1492	0	1083	0	2	0	0
TCGA-62-A46O	LUAD	1454	0	1454	0	1	0	0
TCGA-05-4389	LUAD	1369	1	1369	1	1	0	0
TCGA-38-4632	LUAD	1357	0	680	0	3	0	0
TCGA-44-2655	LUAD	1324	1	1009	0	1	0	0
TCGA-64-5778	LUAD	1305	1	1168	0	1	1	0
TCGA-62-8397	LUAD	1289	1	1289	1	2	0	0
TCGA-62-8395	LUAD	1216	1	395	0	2	0	0
TCGA-62-A470	LUAD	1194	0	1194	0	1	0	0
TCGA-38-4627	LUAD	1147	0	1147	0	1	0	0
TCGA-05-4390	LUAD	1126	1	395	0	1	1	0
TCGA-38-4630	LUAD	1073	0	524	0	1	0	1
TCGA-05-4424	LUAD	913	1	153	0	2	0	1
TCGA-05-4420	LUAD	912	1	912	1	1	0	0
TCGA-05-5425	LUAD	882	1	486	0	2	1	1
TCGA-38-4629	LUAD	864	0	379	0	2	0	0
TCGA-64-5779	LUAD	864	1	795	0	3	1	1
TCGA-05-4427	LUAD	791	1	791	1	2	1	0
TCGA-05-4430	LUAD	761	1	761	1	1	0	0
TCGA-05-4432	LUAD	761	1	761	1	2	1	0
TCGA-05-4397	LUAD	731	0	731	0	2	0	0
TCGA-05-4433	LUAD	730	1	730	1	1	0	0
TCGA-69-7763	LUAD	690	1	690	1	1	0	0
TCGA-05-5428	LUAD	670	1	670	1	1	1	1
TCGA-05-4425	LUAD	669	1	669	1	2	1	0
TCGA-05-4405	LUAD	610	1	610	1	1	0	0
TCGA-67-3771	LUAD	610	1	610	1	1	0	0
TCGA-05-4382	LUAD	607	1	607	1	1	0	1
TCGA-62-A46P	LUAD	594	0	594	0	1	0	0

44

TCGA-05-4403	LUAD	578	1	578	1	1	0	0
TCGA-05-4434	LUAD	457	0	457	0	4	0	0
TCGA-05-5420	LUAD	457	1	245	0	3	0	0
TCGA-05-4417	LUAD	455	1	455	1	1	0	0
TCGA-38-6178	LUAD	448	1	448	1	3	1	0
TCGA-62-8398	LUAD	444	0	444	0	3	1	0
TCGA-67-3773	LUAD	427	1	427	1	1	0	0
TCGA-05-4384	LUAD	426	1	183	0	3	1	1
TCGA-67-6217	LUAD	422	1	296	0	2	0	0
TCGA-62-A46Y	LUAD	414	0	414	0	3	1	1
TCGA-69-7764	LUAD	414	1	414	1	1	0	0
TCGA-67-3774	LUAD	385	1	385	1	1	0	0
TCGA-05-4422	LUAD	365	1	365	1	1	0	0
TCGA-38-4631	LUAD	354	0	354	0	1	0	1
TCGA-05-4396	LUAD	303	0	303	0	4	0	0
TCGA-05-5429	LUAD	275	0	275	0	4	0	0
TCGA-05-4418	LUAD	274	0	274	0	4	0	0
TCGA-35-5375	LUAD	264	1	264	1	3	0	0
TCGA-05-4402	LUAD	244	0	244	0	2	1	0
TCGA-69-7973	LUAD	230	1	230	1	1	1	0
TCGA-35-4122	LUAD	225	1	225	1	1	0	0
TCGA-69-A59K	LUAD	214	1	214	1	2	1	0
TCGA-69-7760	LUAD	202	1	202	1	2	1	0
TCGA-69-7974	LUAD	184	1	184	1	3	1	1
TCGA-35-4123	LUAD	182	1	182	1	1	0	0
TCGA-69-7765	LUAD	165	1	165	1	3	1	0
TCGA-05-5423	LUAD	151	1	151	1	2	0	0
TCGA-67-6216	LUAD	141	1	141	1	1	0	0
TCGA-62-8394	LUAD	139	0	139	0	4	1	0
TCGA-05-4250	LUAD	121	0	121	0	3	0	0
TCGA-05-4415	LUAD	91	0	60	0	4	0	0
TCGA-69-7979	LUAD	89	1	89	1	1	0	0
TCGA-05-5715	LUAD	62	1	62	1	1	0	0
TCGA-64-5775	LUAD	62	0	62	0	3	0	0
TCGA-67-3770	LUAD	31	1	31	1	1	0	0
TCGA-35-3615	LUAD	14	1	14	1	1	0	0
TCGA-05-4395	LUAD	0	0	0	0	4	0	0
TCGA-05-4410	LUAD	0	1	0	1	1	0	0
TCGA-67-4679	LUAD	0	1	0	1	2	0	0
TCGA-CS-5390	LGG	1825	1	1825	1	NA	1	1
TCGA-DB-5270	LGG	1825	1	1825	1	NA	1	1
TCGA-DB-5273	LGG	1825	1	1825	1	NA	1	1
TCGA-DB-5274	LGG	1825	1	1825	1	NA	1	1
TCGA-DB-5276	LGG	1825	1	1825	1	NA	1	1
TCGA-DB-5281	LGG	1825	1	1825	1	NA	1	1
TCGA-DU-5870	LGG	1825	1	1825	1	NA	0	1
TCGA-DU-6396	LGG	1825	1	106	0	NA	1	1
TCGA-DU-6399	LGG	1825	1	1629	0	NA	0	1
TCGA-DU-6401	LGG	1825	1	1825	1	NA	1	1
TCGA-DU-6407	LGG	1825	1	1825	1	NA	0	1
TCGA-DU-7007	LGG	1825	1	1825	1	NA	0	0
TCGA-DU-7008	LGG	1825	1	330	0	NA	0	1
TCGA-DU-7009	LGG	1825	1	1825	1	NA	0	1
TCGA-DU-7294	LGG	1825	1	1825	1	NA	0	0
TCGA-DU-7300	LGG	1825	1	317	0	NA	0	1
TCGA-DU-7302	LGG	1825	1	1374	0	NA	0	0
TCGA-E1-5303	LGG	1825	1	156	0	NA	1	1
TCGA-E1-5305	LGG	1825	1	1604	0	NA	1	1
TCGA-E1-5311	LGG	1825	1	1825	1	NA	1	1
TCGA-E1-5318	LGG	1825	1	362	0	NA	1	1
TCGA-E1-5319	LGG	1825	1	923	0	NA	1	1
TCGA-E1-5322	LGG	1825	1	1085	0	NA	1	1
TCGA-HT-7480	LGG	1825	1	1825	1	NA	1	1
TCGA-HT-7604	LGG	1825	1	1825	1	NA	0	1
TCGA-E1-5307	LGG	1762	0	1452	0	NA	1	1
TCGA-HT-7611	LGG	1752	1	1752	1	NA	0	0
TCGA-DU-6393	LGG	1585	0	1585	0	NA	1	1
TCGA-DB-5277	LGG	1547	0	1156	0	NA	1	1
TCGA-HT-7858	LGG	1540	1	1540	1	NA	0	1
TCGA-E1-5302	LGG	1525	0	1242	0	NA	1	1

TCGA-DU-6395	LGG	1491	0	1197	0	NA	1	1
TCGA-DB-5275	LGG	1458	1	1458	1	NA	1	1
TCGA-FG-5962	LGG	1453	1	1453	1	NA	1	1
TCGA-DU-6397	LGG	1401	0	837	0	NA	1	1
TCGA-HT-7681	LGG	1359	1	1359	1	NA	0	0
TCGA-DB-5279	LGG	1354	1	695	0	NA	0	1
TCGA-DU-7299	LGG	1339	0	675	0	NA	0	1
TCGA-CS-4942	LGG	1335	0	1184	0	NA	1	1
TCGA-IK-8125	LGG	1301	1	1301	1	NA	1	1
TCGA-HT-7686	LGG	1300	1	1300	1	NA	1	1
TCGA-DU-7306	LGG	1277	1	1250	0	NA	1	1
TCGA-E1-5304	LGG	1251	0	903	0	NA	1	1
TCGA-CS-5393	LGG	1222	1	1222	1	NA	1	1
TCGA-HW-7491	LGG	1222	1	1222	1	NA	1	0
TCGA-HT-7470	LGG	1220	0	1220	0	NA	1	1
TCGA-FG-7637	LGG	1219	1	1219	1	NA	0	0
TCGA-HT-7854	LGG	1201	1	1147	0	NA	0	1
TCGA-HT-8018	LGG	1152	0	1152	0	NA	0	1
TCGA-HT-7874	LGG	1130	1	1130	1	NA	1	1
TCGA-FG-5965	LGG	1120	0	715	0	NA	1	1
TCGA-DB-5280	LGG	1112	1	1112	1	NA	0	0
TCGA-FG-5964	LGG	1045	1	1045	1	NA	0	1
TCGA-FG-8191	LGG	992	1	992	1	NA	1	1
TCGA-DH-5141	LGG	968	1	968	1	NA	1	1
TCGA-HT-7688	LGG	964	1	964	1	NA	1	1
TCGA-DU-7018	LGG	933	0	338	0	NA	0	0
TCGA-DH-5142	LGG	922	1	922	1	NA	1	1
TCGA-DB-A4XB	LGG	919	1	919	1	NA	1	1
TCGA-DU-7019	LGG	800	1	800	1	NA	1	1
TCGA-DU-7301	LGG	788	0	366	0	NA	0	1
TCGA-FG-6690	LGG	760	1	760	1	NA	0	1
TCGA-CS-6188	LGG	725	1	647	0	NA	0	1
TCGA-DU-8161	LGG	722	0	111	0	NA	1	1
TCGA-HT-7873	LGG	718	1	718	1	NA	0	1
TCGA-DU-7304	LGG	709	0	309	0	NA	0	1
TCGA-HT-7603	LGG	705	1	705	1	NA	0	1
TCGA-FG-7638	LGG	686	1	407	0	NA	1	1
TCGA-DU-6394	LGG	682	0	353	0	NA	1	1
TCGA-HT-7608	LGG	671	1	671	1	NA	0	0
TCGA-HW-8319	LGG	660	1	660	1	NA	1	1
TCGA-DU-8164	LGG	651	1	651	1	NA	1	0
TCGA-CS-5395	LGG	639	0	287	0	NA	1	1
TCGA-DU-8163	LGG	629	1	509	0	NA	1	1
TCGA-FG-7643	LGG	611	1	254	0	NA	0	0
TCGA-FG-8187	LGG	611	1	611	1	NA	0	0
TCGA-DH-5140	LGG	607	0	607	0	NA	1	1
TCGA-DU-6405	LGG	605	0	486	0	NA	1	1
TCGA-HW-7487	LGG	605	1	605	1	NA	1	0
TCGA-HW-8321	LGG	596	1	596	1	NA	1	1
TCGA-HT-7855	LGG	585	1	585	1	NA	1	1
TCGA-HW-7490	LGG	585	1	585	1	NA	0	0
TCGA-DU-8165	LGG	582	1	582	1	NA	1	1
TCGA-IK-7675	LGG	578	0	123	0	NA	1	1
TCGA-DU-5871	LGG	576	1	576	1	NA	0	1
TCGA-DB-A4XA	LGG	573	1	573	1	NA	0	1
TCGA-FG-6688	LGG	571	1	405	0	NA	1	1
TCGA-FG-6692	LGG	561	0	561	0	NA	1	1
TCGA-FG-A4MW	LGG	559	0	226	0	NA	1	1
TCGA-CS-4943	LGG	552	1	552	1	NA	1	0
TCGA-DU-5847	LGG	548	1	548	1	NA	1	1
TCGA-CS-6290	LGG	546	1	546	1	NA	1	1
TCGA-FG-7636	LGG	544	1	544	1	NA	1	1
TCGA-HW-8322	LGG	542	1	542	1	NA	1	0
TCGA-CS-6186	LGG	538	0	188	0	NA	1	1
TCGA-HT-7693	LGG	533	1	533	1	NA	0	1
TCGA-DU-5872	LGG	532	1	265	0	NA	1	1
TCGA-DU-5851	LGG	531	1	531	1	NA	1	1
TCGA-HT-7475	LGG	530	1	530	1	NA	1	1
TCGA-HT-7606	LGG	526	1	526	1	NA	1	1
TCGA-DU-6406	LGG	512	0	512	0	NA	1	1

TCGA-HT-7473	LGG	503	1	503	1	NA	0	1
TCGA-HT-7677	LGG	494	1	494	1	NA	1	1
TCGA-HT-8011	LGG	494	1	278	0	NA	1	1
TCGA-FG-8186	LGG	487	1	487	1	NA	0	1
TCGA-HT-8564	LGG	478	1	120	0	NA	1	1
TCGA-DU-8167	LGG	471	1	471	1	NA	0	1
TCGA-FG-7634	LGG	467	1	467	1	NA	0	0
TCGA-DU-5874	LGG	461	1	461	1	NA	1	0
TCGA-FG-8188	LGG	455	1	384	0	NA	0	1
TCGA-HT-7689	LGG	455	1	455	1	NA	1	1
TCGA-FG-6689	LGG	454	1	119	0	NA	1	1
TCGA-DU-5849	LGG	443	1	443	1	NA	1	0
TCGA-HT-7695	LGG	442	1	442	1	NA	1	1
TCGA-DH-5143	LGG	438	1	438	1	NA	1	1
TCGA-EZ-7264	LGG	436	1	436	1	NA	0	0
TCGA-HT-7620	LGG	434	1	280	0	NA	1	1
TCGA-DU-8168	LGG	431	1	431	1	NA	1	1
TCGA-HT-8110	LGG	419	1	419	1	NA	0	1
TCGA-DU-5853	LGG	407	1	407	1	NA	1	1
TCGA-CS-6665	LGG	378	1	378	1	NA	0	1
TCGA-HT-8104	LGG	372	1	372	1	NA	0	1
TCGA-DU-6403	LGG	354	0	354	0	NA	1	1
TCGA-HT-7469	LGG	351	0	92	0	NA	1	1
TCGA-DU-7006	LGG	349	0	349	0	NA	0	1
TCGA-HT-7884	LGG	343	1	343	1	NA	1	1
TCGA-CS-4944	LGG	323	1	323	1	NA	0	1
TCGA-CS-5396	LGG	303	1	303	1	NA	1	1
TCGA-DU-7013	LGG	269	0	187	0	NA	1	1
TCGA-DU-5854	LGG	257	1	202	0	NA	0	1
TCGA-HW-7489	LGG	253	1	253	1	NA	0	0
TCGA-CS-6668	LGG	244	1	244	1	NA	0	0
TCGA-DH-5144	LGG	244	1	244	1	NA	0	1
TCGA-DU-6410	LGG	242	1	242	1	NA	1	0
TCGA-DU-7292	LGG	242	0	91	0	NA	0	1
TCGA-CS-4941	LGG	234	0	9	0	NA	1	1
TCGA-DU-6402	LGG	214	0	103	0	NA	1	1
TCGA-HT-7694	LGG	210	1	210	1	NA	0	1
TCGA-DU-5855	LGG	207	1	207	1	NA	1	1
TCGA-DU-5852	LGG	205	0	24	0	NA	1	1
TCGA-HT-7468	LGG	203	1	203	1	NA	1	0
TCGA-CS-6670	LGG	201	1	201	1	NA	1	1
TCGA-HT-7684	LGG	184	1	184	1	NA	0	0
TCGA-HT-8109	LGG	169	1	169	1	NA	0	1
TCGA-DU-8158	LGG	155	0	155	0	NA	1	1
TCGA-HT-7601	LGG	153	1	153	1	NA	1	1
TCGA-CS-4938	LGG	143	1	143	1	NA	0	0
TCGA-HT-7605	LGG	139	1	139	1	NA	0	0
TCGA-HW-7495	LGG	131	1	131	1	NA	0	0
TCGA-HT-7474	LGG	114	1	114	1	NA	0	0
TCGA-HT-7882	LGG	113	0	113	0	NA	0	0
TCGA-HT-7879	LGG	112	1	112	1	NA	1	1
TCGA-HT-7607	LGG	96	0	96	0	NA	0	0
TCGA-HT-7692	LGG	90	1	90	1	NA	0	1
TCGA-DU-7309	LGG	84	1	84	1	NA	0	1
TCGA-HT-8108	LGG	76	1	76	1	NA	0	0
TCGA-HT-8010	LGG	50	1	50	1	NA	0	0
TCGA-DU-6400	LGG	37	0	37	0	NA	0	0
TCGA-HT-7860	LGG	15	1	15	1	NA	0	0
TCGA-HT-7616	LGG	7	0	7	0	NA	0	0
TCGA-HT-7471	LGG	4	1	4	1	NA	0	0
TCGA-CS-5394	LGG	3	1	3	1	NA	0	0
TCGA-HT-7467	LGG	3	1	3	1	NA	0	0
TCGA-HT-7687	LGG	3	1	3	1	NA	0	0
TCGA-HT-7690	LGG	3	1	3	1	NA	0	0
TCGA-HT-7472	LGG	1	1	1	1	NA	0	0
TCGA-A3-3357	KIRC	1825	1	1825	1	1	0	0
TCGA-A3-3367	KIRC	1825	1	1825	1	1	0	0
TCGA-AK-3427	KIRC	1825	1	1825	1	1	0	0
TCGA-B0-4945	KIRC	1825	1	1825	1	1	0	0
TCGA-BP-4760	KIRC	1825	1	1457	0	1	0	0

TCGA-BP-4964	KIRC	1825	1	1825	1	1	0	0
TCGA-BP-5180	KIRC	1825	1	1825	1	1	0	0
TCGA-B0-4842	KIRC	1724	0	250	0	2	0	0
TCGA-A3-3376	KIRC	1696	0	1696	0	1	0	0
TCGA-A3-3373	KIRC	1621	1	1621	1	1	0	0
TCGA-B0-5098	KIRC	1584	0	1584	0	1	0	0
TCGA-A3-3320	KIRC	1508	1	1508	1	1	0	0
TCGA-A3-3316	KIRC	1493	1	1493	1	1	0	0
TCGA-A3-3317	KIRC	1491	1	560	0	1	0	0
TCGA-A3-3322	KIRC	1478	1	1478	1	1	0	0
TCGA-AK-3444	KIRC	1471	1	1471	1	1	0	0
TCGA-AK-3443	KIRC	1423	1	1423	1	1	0	0
TCGA-AK-3453	KIRC	1397	1	1397	1	1	1	0
TCGA-B0-5077	KIRC	1317	0	1317	0	1	0	0
TCGA-A3-3374	KIRC	1314	1	1314	1	1	0	0
TCGA-AS-3777	KIRC	1238	1	1238	1	1	0	0
TCGA-AK-3447	KIRC	1217	1	1217	1	1	0	0
TCGA-A3-3311	KIRC	1191	0	1191	0	1	0	0
TCGA-A3-3326	KIRC	1137	1	1137	1	1	0	0
TCGA-A3-3319	KIRC	1130	1	1130	1	1	0	0
TCGA-A3-3323	KIRC	1106	1	1106	1	1	0	0
TCGA-B2-3924	KIRC	1092	1	1092	1	1	0	0
TCGA-B0-5083	KIRC	1045	0	1045	0	1	0	0
TCGA-B0-4827	KIRC	885	0	668	0	2	0	1
TCGA-A3-3365	KIRC	873	1	873	1	1	0	0
TCGA-A3-3383	KIRC	861	1	861	1	1	0	0
TCGA-B8-5163	KIRC	822	1	822	1	2	0	0
TCGA-B0-5115	KIRC	797	1	75	0	2	1	0
TCGA-B0-5085	KIRC	770	0	770	0	2	0	0
TCGA-B8-5165	KIRC	737	1	737	1	1	0	0
TCGA-A3-3313	KIRC	735	0	735	0	1	0	0
TCGA-A3-3372	KIRC	735	1	735	1	2	0	0
TCGA-BP-5192	KIRC	714	1	714	1	1	0	0
TCGA-AK-3455	KIRC	683	0	683	0	2	0	0
TCGA-B0-5097	KIRC	665	1	359	0	2	0	1
TCGA-B8-5158	KIRC	636	1	636	1	3	0	0
TCGA-A3-3382	KIRC	574	1	514	0	1	0	0
TCGA-A3-3380	KIRC	567	1	567	1	1	0	0
TCGA-B0-5088	KIRC	563	0	563	0	1	0	0
TCGA-EU-5904	KIRC	551	1	551	1	1	0	0
TCGA-B8-5545	KIRC	522	1	522	1	1	0	0
TCGA-B8-4146	KIRC	511	1	511	1	1	0	0
TCGA-B0-5099	KIRC	485	0	485	0	2	0	0
TCGA-B0-5092	KIRC	459	0	459	0	1	0	0
TCGA-B0-4823	KIRC	454	0	454	0	1	0	0
TCGA-AK-3465	KIRC	369	1	369	1	1	0	0
TCGA-A3-3363	KIRC	319	1	319	1	1	0	0
TCGA-B0-5095	KIRC	245	0	245	0	2	0	0
TCGA-EU-5906	KIRC	206	1	206	1	1	0	0
TCGA-B4-5836	KIRC	141	1	141	1	1	0	0
TCGA-EU-5907	KIRC	127	1	127	1	2	0	0
TCGA-EU-5905	KIRC	119	1	119	1	1	0	0
TCGA-B0-5096	KIRC	68	0	68	0	3	0	0
TCGA-B2-4098	KIRC	51	0	51	0	1	0	0
TCGA-AS-3778	KIRC	43	1	43	1	1	0	0
TCGA-B8-5162	KIRC	36	1	36	1	1	1	0
TCGA-B8-5164	KIRC	26	1	26	1	2	0	0
TCGA-A3-3308	KIRC	16	1	16	1	2	0	0
TCGA-B4-5843	KIRC	11	1	11	1	1	0	0
TCGA-B4-5832	KIRC	7	1	7	1	2	0	0
TCGA-BB-4223	HNSC	1825	1	1825	1	3	1	1
TCGA-BB-8596	HNSC	1825	1	1825	1	3	0	1
TCGA-CR-5243	HNSC	1825	1	1825	1	NA	1	1
TCGA-CV-5430	HNSC	1825	1	783	0	4	1	1
TCGA-CV-5434	HNSC	1825	1	1825	1	4	1	1
TCGA-CV-6933	HNSC	1825	1	1825	1	3	0	0
TCGA-CV-6942	HNSC	1825	1	1825	1	1	0	0
TCGA-CV-7089	HNSC	1825	1	1825	1	4	0	0
TCGA-CV-7090	HNSC	1825	1	1825	1	1	0	0
TCGA-CV-7091	HNSC	1825	1	1825	1	1	0	0

48

TCGA-CV-7178	HNSC	1825	1	1825	1	4	0	0
TCGA-CV-7183	HNSC	1825	1	1825	1	1	0	0
TCGA-CV-7250	HNSC	1825	1	1825	1	3	0	0
TCGA-CV-7411	HNSC	1825	1	1825	1	3	0	0
TCGA-CV-7423	HNSC	1825	1	1825	1	1	0	0
TCGA-CV-7427	HNSC	1825	1	1825	1	1	0	0
TCGA-CV-7432	HNSC	1825	1	1825	1	1	0	0
TCGA-CV-7435	HNSC	1825	1	1825	1	4	0	0
TCGA-CR-6467	HNSC	1777	1	1777	1	2	0	1
TCGA-BA-5153	HNSC	1762	0	1522	0	1	1	1
TCGA-CV-7406	HNSC	1748	0	1748	0	1	0	1
TCGA-CV-7235	HNSC	1724	1	1724	1	1	0	0
TCGA-CV-7425	HNSC	1718	0	1718	0	2	0	0
TCGA-CV-7103	HNSC	1591	0	1591	0	3	0	0
TCGA-CR-6470	HNSC	1521	1	1521	1	1	1	1
TCGA-CR-7404	HNSC	1472	1	234	0	NA	1	1
TCGA-CQ-7063	HNSC	1461	1	1461	1	1	0	0
TCGA-CV-7238	HNSC	1444	1	1444	1	1	0	0
TCGA-CR-7386	HNSC	1430	1	1028	0	4	1	1
TCGA-BA-5152	HNSC	1288	1	1288	1	3	0	1
TCGA-CR-7368	HNSC	1245	1	1245	1	4	1	1
TCGA-CQ-5324	HNSC	1207	1	1207	1	2	0	0
TCGA-CR-6471	HNSC	1202	0	498	0	4	1	1
TCGA-CR-7365	HNSC	1191	1	1191	1	3	1	1
TCGA-BA-4077	HNSC	1134	0	1134	0	3	1	0
TCGA-CV-7242	HNSC	1095	1	1095	1	1	0	0
TCGA-CR-7369	HNSC	1090	0	1090	0	4	0	0
TCGA-CN-4741	HNSC	1086	1	1086	1	3	1	1
TCGA-CN-5360	HNSC	1081	1	1081	1	3	1	1
TCGA-CV-7407	HNSC	1081	0	1081	0	1	0	0
TCGA-CR-7401	HNSC	1077	1	1077	1	1	0	0
TCGA-CQ-6223	HNSC	1057	1	1057	1	1	0	0
TCGA-CR-6472	HNSC	1050	1	1050	1	NA	1	1
TCGA-CV-7422	HNSC	1037	0	1037	0	4	0	0
TCGA-CQ-5331	HNSC	1028	1	1028	1	1	0	0
TCGA-CQ-7065	HNSC	1007	1	230	0	1	1	1
TCGA-CQ-6221	HNSC	1000	1	1000	1	1	0	0
TCGA-CQ-6220	HNSC	985	0	985	0	2	0	0
TCGA-CR-7395	HNSC	930	1	930	1	1	0	0
TCGA-CR-7402	HNSC	911	1	911	1	NA	1	1
TCGA-CR-7390	HNSC	907	1	907	1	3	0	0
TCGA-CQ-7069	HNSC	901	1	901	1	1	0	0
TCGA-CQ-5330	HNSC	896	1	896	1	4	1	1
TCGA-CR-7373	HNSC	889	1	889	1	4	1	1
TCGA-CQ-7071	HNSC	877	1	877	1	2	0	1
TCGA-CQ-6218	HNSC	870	1	870	1	4	1	1
TCGA-CV-6960	HNSC	862	0	862	0	2	0	0
TCGA-CQ-5329	HNSC	841	1	841	1	1	0	0
TCGA-CN-4740	HNSC	839	0	224	0	3	1	1
TCGA-CR-7388	HNSC	823	0	334	0	NA	1	1
TCGA-CQ-6229	HNSC	815	1	815	1	1	0	0
TCGA-CR-5250	HNSC	799	1	799	1	NA	1	1
TCGA-CV-7245	HNSC	797	1	797	1	3	0	0
TCGA-CR-7382	HNSC	796	1	614	0	3	1	1
TCGA-CV-7416	HNSC	763	0	763	0	3	1	1
TCGA-BA-5556	HNSC	725	1	725	1	1	0	0
TCGA-BA-5151	HNSC	722	1	517	0	3	0	1
TCGA-CV-7415	HNSC	695	0	695	0	4	0	0
TCGA-CN-4731	HNSC	693	1	243	0	4	1	1
TCGA-CQ-7068	HNSC	693	1	693	1	1	0	1
TCGA-CV-6939	HNSC	666	0	666	0	4	0	0
TCGA-CV-7177	HNSC	663	0	663	0	1	0	0
TCGA-BA-6869	HNSC	644	1	644	1	2	0	1
TCGA-BB-8601	HNSC	624	1	624	1	3	0	0
TCGA-CV-6937	HNSC	624	0	624	0	1	0	0
TCGA-BA-5557	HNSC	623	1	623	1	1	1	1
TCGA-CN-4728	HNSC	613	1	613	1	4	1	1
TCGA-CR-7380	HNSC	606	0	561	0	3	1	1
TCGA-CV-7433	HNSC	601	0	601	0	4	0	0
TCGA-CV-5436	HNSC	584	0	584	0	4	0	0

TCGA-CV-7247	HNSC	577	0	577	0	2	0	0
TCGA-CV-7263	HNSC	560	0	560	0	1	0	0
TCGA-BB-4228	HNSC	558	1	558	1	2	0	1
TCGA-CN-4737	HNSC	541	1	541	1	3	1	1
TCGA-CN-A63U	HNSC	526	1	526	1	4	0	1
TCGA-BA-A4IF	HNSC	523	1	523	1	NA	1	1
TCGA-CR-7383	HNSC	521	0	454	0	1	1	1
TCGA-CV-7248	HNSC	521	0	521	0	4	0	0
TCGA-BA-5555	HNSC	520	1	248	0	4	0	0
TCGA-CR-6477	HNSC	514	1	514	1	NA	1	1
TCGA-CN-5356	HNSC	512	1	512	1	2	0	0
TCGA-CV-7430	HNSC	495	0	495	0	3	0	0
TCGA-CN-5364	HNSC	493	0	493	0	4	1	1
TCGA-CN-6989	HNSC	490	1	436	0	4	1	1
TCGA-CN-5355	HNSC	488	1	488	1	3	0	0
TCGA-BA-4074	HNSC	462	0	396	0	3	0	1
TCGA-CN-4730	HNSC	462	1	462	1	4	0	0
TCGA-CV-6950	HNSC	459	0	459	0	4	0	0
TCGA-CQ-6228	HNSC	456	0	273	0	2	0	1
TCGA-BA-6870	HNSC	451	0	451	0	NA	1	1
TCGA-CN-A49B	HNSC	447	1	447	1	3	0	1
TCGA-CN-6013	HNSC	433	1	323	0	4	1	1
TCGA-CN-6996	HNSC	432	1	350	0	4	1	1
TCGA-BA-4076	HNSC	415	0	286	0	NA	0	1
TCGA-CQ-6225	HNSC	403	0	180	0	2	0	0
TCGA-CN-6997	HNSC	398	1	279	0	4	1	1
TCGA-CN-4742	HNSC	397	0	397	0	4	1	1
TCGA-CN-4736	HNSC	395	0	209	0	1	1	1
TCGA-CN-6992	HNSC	394	1	394	1	4	1	1
TCGA-CV-7104	HNSC	393	0	393	0	3	0	0
TCGA-CR-7389	HNSC	392	1	392	1	NA	1	1
TCGA-CN-6019	HNSC	391	1	391	1	3	1	1
TCGA-CV-7097	HNSC	385	0	385	0	1	0	0
TCGA-CN-A641	HNSC	367	1	367	1	4	1	1
TCGA-CR-6480	HNSC	362	1	362	1	NA	1	1
TCGA-CN-5366	HNSC	360	0	276	0	4	1	1
TCGA-CR-5247	HNSC	358	1	358	1	NA	1	1
TCGA-CN-6998	HNSC	357	0	244	0	4	1	1
TCGA-CN-5365	HNSC	351	0	351	0	4	0	0
TCGA-CN-6994	HNSC	350	1	350	1	3	0	0
TCGA-CN-6024	HNSC	337	0	156	0	4	0	0
TCGA-CV-7180	HNSC	327	0	327	0	1	0	0
TCGA-CN-6988	HNSC	318	1	318	1	4	0	0
TCGA-CQ-5332	HNSC	317	0	317	0	2	0	0
TCGA-CN-6016	HNSC	316	1	316	1	4	1	1
TCGA-CV-6935	HNSC	295	0	295	0	4	0	0
TCGA-CV-7413	HNSC	294	0	294	0	1	0	0
TCGA-CN-5374	HNSC	290	1	290	1	3	1	1
TCGA-CR-6493	HNSC	282	0	282	0	4	0	0
TCGA-CN-6022	HNSC	281	0	101	0	4	0	1
TCGA-CR-7377	HNSC	279	0	279	0	4	0	0
TCGA-BB-4224	HNSC	278	1	175	0	3	1	1
TCGA-BA-4078	HNSC	276	0	276	0	NA	0	1
TCGA-CV-7100	HNSC	274	0	274	0	2	0	0
TCGA-CN-5370	HNSC	259	0	123	0	3	1	1
TCGA-CN-5363	HNSC	253	0	53	0	4	0	0
TCGA-CV-7099	HNSC	243	0	243	0	1	0	0
TCGA-BA-A6DF	HNSC	238	0	238	0	3	0	1
TCGA-CN-4734	HNSC	227	1	227	1	1	0	1
TCGA-CV-7434	HNSC	218	0	218	0	4	0	0
TCGA-CN-6020	HNSC	205	0	205	0	2	0	1
TCGA-CN-4727	HNSC	194	1	194	1	3	1	1
TCGA-CR-7399	HNSC	181	1	181	1	4	0	1
TCGA-CN-A63Y	HNSC	175	1	175	1	1	0	0
TCGA-CN-4729	HNSC	156	1	156	1	2	0	0
TCGA-CR-7398	HNSC	156	1	156	1	1	0	0
TCGA-CV-7252	HNSC	151	0	151	0	3	0	0
TCGA-CV-6938	HNSC	144	0	144	0	1	0	0
TCGA-CV-7236	HNSC	144	0	144	0	4	0	0
TCGA-CN-4726	HNSC	142	0	79	0	4	1	1

TCGA-CQ-6227	HNSC	129	0	129	0	4	0	0
TCGA-BA-6873	HNSC	122	1	66	0	4	1	1
TCGA-CN-6995	HNSC	112	0	112	0	3	0	0
TCGA-BA-6871	HNSC	108	0	108	0	NA	0	1
TCGA-CV-7429	HNSC	107	0	107	0	4	0	0
TCGA-CR-7370	HNSC	105	1	105	1	NA	0	1
TCGA-CR-7371	HNSC	94	0	94	0	3	0	0
TCGA-CV-6961	HNSC	76	0	76	0	1	0	0
TCGA-CV-6934	HNSC	65	0	65	0	4	0	0
TCGA-CV-7102	HNSC	56	0	56	0	4	0	0
TCGA-CN-6018	HNSC	45	1	45	1	4	0	0
TCGA-CR-7374	HNSC	30	1	30	1	NA	0	0
TCGA-C9-A47Z	HNSC	5	1	5	1	2	0	0
TCGA-C9-A480	HNSC	4	1	4	1	2	0	0
TCGA-CV-7421	HNSC	2	0	2	0	3	0	0
TCGA-32-2498	GBM	NA	NA	NA	NA	NA	0	0
TCGA-76-6283	GBM	NA	NA	NA	NA	NA	0	0
TCGA-06-0178	GBM	1825	1	192	0	NA	1	1
TCGA-06-0184	GBM	1825	1	1276	0	NA	1	1
TCGA-06-0185	GBM	1825	1	711	0	NA	1	1
TCGA-06-6693	GBM	1825	1	1825	1	NA	0	0
TCGA-14-1450	GBM	1788	1	826	0	NA	1	1
TCGA-06-0241	GBM	1481	0	196	0	NA	1	1
TCGA-06-0744	GBM	1426	0	1277	0	NA	1	1
TCGA-06-0151	GBM	1417	0	1417	0	NA	1	1
TCGA-06-0876	GBM	1405	1	424	0	NA	1	1
TCGA-06-0188	GBM	1356	0	310	0	NA	1	1
TCGA-27-1834	GBM	1233	0	335	0	NA	1	1
TCGA-06-0879	GBM	1229	0	699	0	NA	1	1
TCGA-06-0192	GBM	1185	0	648	0	NA	1	1
TCGA-12-0619	GBM	1062	0	203	0	NA	1	1
TCGA-14-0871	GBM	880	0	880	0	NA	0	1
TCGA-06-0187	GBM	828	0	531	0	NA	1	1
TCGA-12-0688	GBM	811	0	228	0	NA	1	1
TCGA-06-0132	GBM	771	0	482	0	NA	1	1
TCGA-27-1833	GBM	737	0	469	0	NA	1	1
TCGA-06-0216	GBM	735	0	175	0	NA	1	1
TCGA-76-6286	GBM	638	0	180	0	NA	1	1
TCGA-74-6575	GBM	636	1	93	0	NA	1	1
TCGA-06-0882	GBM	632	0	213	0	NA	1	1
TCGA-06-0240	GBM	621	0	621	0	NA	1	1
TCGA-06-0168	GBM	598	0	461	0	NA	1	1
TCGA-08-0386	GBM	548	0	427	0	NA	1	1
TCGA-14-1823	GBM	543	0	140	0	NA	1	1
TCGA-81-5911	GBM	539	1	277	0	NA	1	1
TCGA-16-0848	GBM	535	0	129	0	NA	1	1
TCGA-12-0615	GBM	467	0	160	0	NA	1	1
TCGA-06-1806	GBM	466	0	466	0	NA	1	1
TCGA-06-0214	GBM	457	0	48	0	NA	1	1
TCGA-02-0047	GBM	448	0	57	0	NA	0	1
TCGA-12-0616	GBM	448	0	398	0	NA	1	1
TCGA-74-6578	GBM	436	1	222	0	NA	1	1
TCGA-06-0686	GBM	432	0	160	0	NA	1	1
TCGA-06-0154	GBM	424	0	208	0	NA	1	1
TCGA-15-0742	GBM	419	0	232	0	NA	1	1
TCGA-06-0237	GBM	415	0	415	0	NA	1	1
TCGA-06-0238	GBM	405	0	311	0	NA	1	1
TCGA-12-0618	GBM	395	0	395	0	NA	1	1
TCGA-06-6697	GBM	391	1	306	0	NA	1	1
TCGA-06-0644	GBM	384	0	85	0	NA	1	1
TCGA-41-6646	GBM	379	0	200	0	NA	1	1
TCGA-14-0740	GBM	364	0	364	0	NA	0	1
TCGA-28-5211	GBM	358	1	225	0	NA	1	1
TCGA-06-0167	GBM	347	0	347	0	NA	1	1
TCGA-76-6280	GBM	346	0	108	0	NA	1	1
TCGA-14-0789	GBM	342	0	105	0	NA	1	1
TCGA-06-0158	GBM	329	0	90	0	NA	1	1
TCGA-06-0165	GBM	324	0	324	0	NA	1	1
TCGA-06-0648	GBM	298	0	202	0	NA	1	1
TCGA-76-6662	GBM	282	1	205	0	NA	1	1

TCGA-06-6695	GBM	253	1	133	0	NA	1	1
TCGA-74-6581	GBM	250	1	250	1	NA	1	1
TCGA-26-6173	GBM	241	1	241	1	NA	1	1
TCGA-06-0745	GBM	239	0	92	0	NA	1	1
TCGA-76-6664	GBM	237	1	237	1	NA	1	0
TCGA-76-6663	GBM	235	1	235	1	NA	1	1
TCGA-06-0209	GBM	232	0	232	0	NA	0	1
TCGA-14-1825	GBM	232	0	82	0	NA	0	1
TCGA-74-6584	GBM	228	1	91	0	NA	1	1
TCGA-06-0195	GBM	225	0	147	0	NA	1	1
TCGA-06-6694	GBM	224	0	224	0	NA	0	0
TCGA-06-0878	GBM	218	1	66	0	NA	1	1
TCGA-14-1829	GBM	218	1	218	1	NA	1	1
TCGA-06-0645	GBM	175	0	175	0	NA	0	0
TCGA-06-0646	GBM	175	0	90	0	NA	1	1
TCGA-06-0877	GBM	172	0	172	0	NA	0	1
TCGA-14-0817	GBM	164	0	164	0	NA	0	0
TCGA-06-6388	GBM	159	0	85	0	NA	1	1
TCGA-27-1830	GBM	154	0	124	0	NA	1	1
TCGA-76-6657	GBM	153	0	135	0	NA	1	1
TCGA-06-6701	GBM	151	1	151	1	NA	1	1
TCGA-76-6656	GBM	147	0	147	0	NA	1	1
TCGA-06-6698	GBM	145	1	145	1	NA	1	1
TCGA-06-6700	GBM	145	1	145	1	NA	1	1
TCGA-02-0003	GBM	144	0	40	0	NA	1	1
TCGA-19-5953	GBM	144	0	119	0	NA	0	0
TCGA-06-0173	GBM	136	0	136	0	NA	0	0
TCGA-74-6577	GBM	132	1	132	0	NA	1	1
TCGA-16-0861	GBM	131	1	94	0	NA	1	1
TCGA-16-0846	GBM	119	0	119	0	NA	0	0
TCGA-12-0692	GBM	111	0	35	0	NA	1	0
TCGA-74-6573	GBM	105	0	105	0	NA	1	1
TCGA-06-0174	GBM	98	0	47	0	NA	1	1
TCGA-06-0157	GBM	97	0	97	0	NA	0	1
TCGA-14-0862	GBM	88	0	88	0	NA	0	0
TCGA-02-0033	GBM	86	0	32	0	NA	0	1
TCGA-06-0747	GBM	82	0	82	0	NA	1	1
TCGA-06-0749	GBM	82	0	82	0	NA	1	1
TCGA-02-0055	GBM	76	0	6	0	NA	1	1
TCGA-26-6174	GBM	71	1	71	1	NA	1	1
TCGA-14-0787	GBM	68	0	68	0	NA	0	0
TCGA-06-0649	GBM	64	0	64	0	NA	0	0
TCGA-06-6699	GBM	47	1	47	1	NA	1	1
TCGA-14-1395	GBM	42	0	42	0	NA	1	0
TCGA-14-0813	GBM	41	0	41	0	NA	0	0
TCGA-06-0750	GBM	28	0	28	0	NA	0	0
TCGA-14-1043	GBM	24	0	24	0	NA	0	1
TCGA-06-0219	GBM	22	0	22	0	NA	0	0
TCGA-06-0213	GBM	16	0	16	0	NA	0	0
TCGA-76-6661	GBM	7	1	7	1	NA	1	1
TCGA-C5-A1BE	CESC	1825	1	1825	1	1	1	1
TCGA-C5-A1BJ	CESC	1825	1	1825	1	NA	0	1
TCGA-C5-A1BK	CESC	1825	1	1825	1	1	0	0
TCGA-C5-A1BL	CESC	1825	1	1825	1	1	0	1
TCGA-C5-A1BM	CESC	1825	1	1825	1	2	0	1
TCGA-C5-A1M5	CESC	1825	1	1825	1	1	0	1
TCGA-DR-A0ZL	CESC	1825	1	1825	1	1	0	0
TCGA-DS-A0VM	CESC	1825	1	1825	1	1	1	0
TCGA-DS-A0VN	CESC	1825	1	1825	1	1	1	1
TCGA-C5-A1MF	CESC	1617	1	1617	1	1	0	1
TCGA-BI-A0VR	CESC	1505	1	1505	1	2	0	0
TCGA-C5-A1M7	CESC	1409	1	1409	1	1	0	0
TCGA-DR-A0ZM	CESC	1289	1	1289	1	2	1	1
TCGA-C5-A1MN	CESC	1245	0	1245	0	NA	1	1
TCGA-C5-A1MH	CESC	1186	0	1186	0	NA	1	1
TCGA-DS-A0VK	CESC	1118	0	1118	0	1	1	1
TCGA-C5-A1BI	CESC	1112	1	1112	1	1	1	1
TCGA-C5-A1MI	CESC	1083	0	1083	0	1	1	1
TCGA-C5-A1M9	CESC	1065	0	1065	0	3	1	1
TCGA-C5-A1M6	CESC	955	0	955	0	NA	1	1

TCGA-C5-A1M8	CESC	919	1	919	1	1	0	1
TCGA-FU-A23L	CESC	725	1	725	1	1	1	1
TCGA-EX-A1H5	CESC	619	1	619	1	2	0	1
TCGA-C5-A1BF	CESC	570	0	570	0	NA	1	1
TCGA-C5-A0TN	CESC	348	0	348	0	1	1	1
TCGA-C5-A1BN	CESC	166	0	166	0	NA	1	1
TCGA-C5-A1MP	CESC	109	1	109	1	1	0	0
TCGA-DS-A0VL	CESC	81	1	81	1	1	0	0
TCGA-C5-A1MK	CESC	74	0	74	0	NA	1	1
TCGA-FU-A23K	CESC	37	1	37	1	1	0	0
TCGA-C5-A1MQ	CESC	17	1	17	1	1	1	1
TCGA-C5-A1MJ	CESC	14	0	14	0	1	0	0
TCGA-EA-A1QT	CESC	8	1	8	1	1	0	0
TCGA-DK-A1A6	BLCA	1825	1	1825	1	2	0	0
TCGA-DK-A1AD	BLCA	1825	1	1825	1	4	0	0
TCGA-DK-A2I4	BLCA	1825	1	1825	1	2	0	0
TCGA-DK-A2I6	BLCA	1825	1	1825	1	2	0	0
TCGA-DK-A6AV	BLCA	1825	1	1825	1	1	0	0
TCGA-DK-A6B0	BLCA	1825	1	1825	1	1	0	0
TCGA-DK-A6B1	BLCA	1825	1	1825	1	1	0	0
TCGA-FD-A3NA	BLCA	1825	1	1825	1	1	0	0
TCGA-G2-A2EF	BLCA	1825	1	1825	1	NA	1	0
TCGA-FD-A5C1	BLCA	1792	1	1792	1	2	1	0
TCGA-DK-A3IS	BLCA	1529	1	1529	1	1	0	0
TCGA-DK-A3X1	BLCA	1460	1	1460	1	2	0	0
TCGA-FD-A3SQ	BLCA	1423	0	1423	0	4	1	0
TCGA-E5-A2PC	BLCA	1326	1	1326	1	2	1	0
TCGA-BL-A0C8	BLCA	1219	1	1219	1	1	0	0
TCGA-E5-A4U1	BLCA	1181	1	1181	1	1	1	0
TCGA-HQ-A2OE	BLCA	1174	1	1174	1	3	1	0
TCGA-FD-A3B6	BLCA	1005	0	1005	0	1	0	0
TCGA-FD-A3B3	BLCA	974	0	974	0	2	0	0
TCGA-FJ-A3Z7	BLCA	945	1	945	1	4	1	0
TCGA-DK-A6B6	BLCA	933	1	933	1	NA	1	0
TCGA-G2-A2EJ	BLCA	931	1	931	1	NA	1	0
TCGA-K4-A54R	BLCA	842	1	842	1	1	0	0
TCGA-GV-A3QK	BLCA	832	1	832	1	4	1	1
TCGA-K4-A3WS	BLCA	761	1	761	1	2	0	0
TCGA-GC-A3YS	BLCA	758	1	758	1	3	0	0
TCGA-FD-A3SL	BLCA	712	0	712	0	4	1	0
TCGA-DK-A3IU	BLCA	706	0	706	0	1	1	0
TCGA-FD-A43N	BLCA	699	1	699	1	2	0	0
TCGA-FD-A3N5	BLCA	685	0	685	0	1	0	0
TCGA-GV-A3JW	BLCA	649	1	649	1	1	0	1
TCGA-K4-A3WV	BLCA	646	1	646	1	1	0	0
TCGA-GD-A3OS	BLCA	638	1	638	1	NA	1	0
TCGA-FD-A43U	BLCA	636	1	636	1	4	1	0
TCGA-DK-A3WW	BLCA	633	1	633	1	2	1	0
TCGA-BT-A2LD	BLCA	623	0	623	0	3	1	1
TCGA-G2-A3IE	BLCA	612	0	612	0	NA	1	0
TCGA-GV-A3JZ	BLCA	603	1	603	1	4	0	0
TCGA-FD-A3SR	BLCA	602	0	602	0	4	1	0
TCGA-H4-A2HQ	BLCA	590	1	590	1	NA	0	0
TCGA-GV-A3JX	BLCA	581	1	581	1	2	0	0
TCGA-DK-A1AA	BLCA	578	1	578	1	2	1	0
TCGA-DK-A1A7	BLCA	560	1	112	0	4	0	0
TCGA-FD-A3SM	BLCA	547	0	547	0	4	0	0
TCGA-GC-A3WC	BLCA	540	1	540	1	2	0	0
TCGA-DK-A3IQ	BLCA	539	0	539	0	2	1	0
TCGA-DK-A1AF	BLCA	536	1	283	0	4	0	0
TCGA-G2-A3VY	BLCA	536	1	536	1	NA	0	0
TCGA-E7-A541	BLCA	529	1	529	1	1	0	0
TCGA-FJ-A3ZF	BLCA	524	1	524	1	NA	1	0
TCGA-FD-A3B4	BLCA	510	0	510	0	3	1	0
TCGA-E7-A519	BLCA	508	1	508	1	1	0	0
TCGA-DK-A1AE	BLCA	491	1	211	0	2	0	1
TCGA-G2-A2EK	BLCA	485	1	485	1	NA	0	0
TCGA-GC-A3OO	BLCA	481	1	481	1	1	0	0
TCGA-DK-A1AG	BLCA	475	1	475	1	2	0	0
TCGA-K4-A6MB	BLCA	469	1	469	1	3	0	0

53

TCGA-E5-A4TZ	BLCA	467	0	467	0	4	1	1
TCGA-E7-A677	BLCA	443	1	443	1	1	0	0
TCGA-GV-A3JV	BLCA	434	0	434	0	3	0	0
TCGA-GC-A3RD	BLCA	428	1	428	1	2	0	0
TCGA-E7-A678	BLCA	425	1	425	1	2	0	0
TCGA-DK-A3IL	BLCA	413	0	413	0	4	0	0
TCGA-MV-A51V	BLCA	410	1	410	1	2	0	0
TCGA-BT-A0YX	BLCA	400	0	326	0	2	0	0
TCGA-CF-A47T	BLCA	385	0	385	0	1	0	1
TCGA-CF-A47V	BLCA	379	1	379	1	1	0	1
TCGA-CF-A47Y	BLCA	373	1	373	1	1	0	0
TCGA-CF-A47W	BLCA	368	1	368	1	1	0	0
TCGA-GU-A42R	BLCA	344	1	344	1	NA	0	0
TCGA-FD-A5BT	BLCA	335	0	335	0	2	0	0
TCGA-FJ-A3ZE	BLCA	324	0	324	0	NA	0	1
TCGA-GV-A3QI	BLCA	322	1	322	1	2	0	0
TCGA-DK-A3WX	BLCA	321	0	321	0	2	1	1
TCGA-DK-A3IV	BLCA	294	0	294	0	NA	1	0
TCGA-C4-A0EZ	BLCA	273	0	273	0	4	0	0
TCGA-GV-A40E	BLCA	261	0	261	0	NA	1	1
TCGA-GV-A3QH	BLCA	258	0	258	0	NA	1	0
TCGA-FD-A5BY	BLCA	251	1	251	1	2	0	0
TCGA-DK-A2I2	BLCA	237	0	237	0	4	0	0
TCGA-GD-A2C5	BLCA	235	1	235	1	4	1	1
TCGA-G2-A3IB	BLCA	220	0	220	0	NA	0	0
TCGA-CU-A0YR	BLCA	219	1	219	0	3	0	0
TCGA-FJ-A3Z9	BLCA	217	1	217	1	1	1	0
TCGA-FD-A62O	BLCA	216	0	216	0	4	0	0
TCGA-FT-A61P	BLCA	197	1	197	1	4	0	0
TCGA-FD-A62P	BLCA	191	0	191	0	1	0	0
TCGA-FD-A5BX	BLCA	173	0	173	0	3	0	0
TCGA-FD-A3SO	BLCA	168	0	168	0	3	1	0
TCGA-CU-A3KJ	BLCA	166	1	166	1	2	0	0
TCGA-FD-A5BV	BLCA	163	0	163	0	2	0	0
TCGA-CU-A3QU	BLCA	158	1	158	1	2	0	0
TCGA-BT-A3PH	BLCA	142	0	142	0	4	0	0
TCGA-FD-A3B7	BLCA	122	0	122	0	2	0	0
TCGA-FD-A43X	BLCA	110	1	110	1	1	0	0
TCGA-K4-A3WU	BLCA	105	1	105	1	3	0	0
TCGA-GD-A3OQ	BLCA	95	1	95	1	4	0	0
TCGA-K4-A4AB	BLCA	84	1	84	1	3	0	0
TCGA-FD-A62N	BLCA	82	1	82	1	2	0	0
TCGA-E7-A4XJ	BLCA	68	0	68	0	1	0	0
TCGA-GC-A3I6	BLCA	68	1	68	1	2	0	0
TCGA-DK-A3IK	BLCA	67	1	67	1	4	0	0
TCGA-GD-A6C6	BLCA	67	1	67	1	2	0	0
TCGA-C4-A0F0	BLCA	59	1	59	1	1	0	0
TCGA-DK-A2HX	BLCA	55	1	55	1	4	0	0
TCGA-K4-A6FZ	BLCA	55	1	55	1	2	0	0
TCGA-H4-A2HO	BLCA	46	1	46	1	3	0	0
TCGA-E7-A7DV	BLCA	37	1	37	1	4	0	0
TCGA-E7-A5KF	BLCA	20	1	20	1	1	0	0
TCGA-E7-A5KE	BLCA	17	1	17	1	1	0	0
TCGA-CF-A1HS	BLCA	13	1	13	1	2	0	0
TCGA-E7-A3Y1	BLCA	3	1	3	1	NA	0	0
TCGA-CF-A3MF	BLCA	0	1	0	1	2	0	0
TCGA-CF-A3MG	BLCA	0	1	0	1	1	0	0

Supplementary Table 8

Prognostic significance of low/high CNV abundance in an independent dataset. CNVs measured on genome-wide SNP arrays (Affymetrix 6.0) in an independent dataset consisting of 2,010 tumor samples (74 adrenocortical carcinomas, 989 breast invasive carcinomas, 427 colon adenocarcinomas, 65 kidney chromophobes, 162 rectum adenocarcinomas, 108 sarcomas and 185 ovarian serous cystadenocarcinomas) confirm that the presence of CNVs affecting very low or very high fractions of the genome (low/high CNV abundance) is a significant protective factor. Shown are p-values and hazard ratios obtained from univariate Cox models testing the association between low/high CNV abundance and overall survival, within and across cancer types. P-values below 0.05 are marked blue.

Cancer type	Statistic	Low/high CNV abundance
All cancers	p-value	5.60E-05
	hazard ratio	0.27
	# Samples	2010
ACC	p-value	0.47
	hazard ratio	0.53
	# Samples	74
BRCA	p-value	0.09
	hazard ratio	0.32
	# Samples	989
COAD	p-value	0.04
	hazard ratio	0.36
	# Samples	427
KICH	p-value	0.01
	hazard ratio	0.00
	# Samples	65
READ	p-value	0.14
	hazard ratio	0.25
	# Samples	162
SARC	p-value	0.05
	hazard ratio	0.25
	# Samples	108
OV	p-value	0.59
	hazard ratio	0.77
	# Samples	185

Supplementary Table 9

Tumor type specific multivariate Cox models of overall survival. The prognostic significance of clone number and low/high CNV abundance were evaluated in the context of clinical data. One multivariate Cox model was evaluated for each tumor type separately (included covariates vary with tumor type, subject to data availability and model stability). P-values and hazard ratios (HR) associated with differential clone number are shown for each tumor type along with the p-values and hazard ratios of the other covariates included in the multivariate models. The hazard of individuals with a low or high number of clones was calculated relative to the hazard of individuals with an intermediate number of clones (between 3 and 5 clones). P-values below 0.05 are marked green. The magnitude of the hazard ratio is color-coded (yellow: favorable outcome; red: poor outcome; gray: moderate effect). Where variables did not satisfy the proportionality assumption for the Cox model (P<0.05), the corresponding hazard ratios are flagged (*).

Cancer type	Covariate	HR	Log (HR)	P-value
BLCA	1 or 2 vs. 3 clones	1.965	0.675	0.562
BLCA	4 vs. 3 clones	0.778	-0.251	0.819
BLCA	6 or 7 vs. 3 clones	0.248	-1.396	0.108
BLCA	8 or 9 vs. 3 clones	0.169	-1.777	0.060
BLCA	10 or more vs. 3 clones	0.286	-1.253	0.188
BLCA	Age at diagnosis	0.027	-3.608	0.167
BLCA	Low/high CNV abundance	0.006	-5.087	0.033
BLCA	MKI67	5E6(*)	13.149	0.011
BLCA	% Lymphocytes	0.440	-0.820	0.895
BLCA	Grade	0.084	-2.474	0.427
BLCA	Pathologic stage	4.949	1.599	0.078
CESC	5 vs. 4 clones	0.359	-1.025	0.283
CESC	Age at diagnosis	0.680	-0.385	0.886
CESC	Low/high CNV abundance	0.058	-2.848	0.622
CESC	% Lymphocytes	0.045	-3.106	0.056
CESC	Grade	0.086	-2.449	0.319
GBM	1 or 2 vs. 5 clones	0.504	-0.685	0.114
GBM	3 vs. 5 clones	0.634	-0.456	0.340
GBM	4 vs. 5 clones	0.599	-0.512	0.230
GBM	6 or 7 vs. 5 clones	0.613	-0.490	0.254
GBM	8 or 9 vs. 5 clones	0.362	-1.016	0.137
GBM	10 or more vs. 5 clones	0.449	-0.801	0.135
GBM	Age at diagnosis	2.596	0.954	0.242
GBM	% Lymphocytes	1.990	0.688	0.659
HNSC	1 or 2 vs. 4 clones	0.524	-0.646	0.190
HNSC	3 vs. 4 clones	0.582	-0.542	0.237
HNSC	5 vs. 4 clones	0.486	-0.721	0.096
HNSC	6 or 7 vs. 4 clones	0.497	-0.700	0.119
HNSC	8 or 9 vs. 4 clones	0.607	-0.499	0.301
HNSC	10 or more vs. 4 clones	0.205	-1.587	0.017
HNSC	Age at diagnosis	10.533	2.354	0.019
HNSC	Low/high CNV abundance	0.279	-1.277	0.213
HNSC	MKI67	5.584	1.720	0.445

HNSC	% Lymphocytes	0.064	-2.749	0.086
HNSC	Grade	2.998	1.098	0.120
HNSC	Pathologic stage	1.970	0.678	0.056
KIRC	1 or 2 vs. 4 clones	0.197	-1.627	0.112
KIRC	3 vs. 4 clones	0.158	-1.847	0.030
KIRC	5 vs. 4 clones	0.143	-1.947	0.066
KIRC	Age at diagnosis	244.955	5.501	0.048
KIRC	Low/high CNV abundance	13.790	2.624	0.780
KIRC	MKI67	63.115	4.145	0.307
KIRC	Grade	3.049	1.115	0.589
KIRC	Pathologic stage	0.563	-0.575	0.831
LGG	1 or 2 vs. 5 clones	0.954	-0.047	0.936
LGG	3 vs. 5 clones	0.224	-1.496	0.060
LGG	4 vs. 5 clones	0.505	-0.684	0.293
LGG	6 or 7 vs. 5 clones	0.405	-0.903	0.217
LGG	Age at diagnosis	117.919(*)	4.770	5.58E-05
LGG	Low/high CNV abundance	0.084	-2.472	0.173
LGG	MKI67	9.722	2.274	0.082
LGG	Grade	5.691	1.739	0.179
LUAD	1 or 2 vs. 4 clones	0.298	-1.211	0.314
LUAD	3 vs. 4 clones	0.684	-0.380	0.702
LUAD	5 vs. 4 clones	0.385	-0.956	0.396
LUAD	6 or 7 vs. 4 clones	1.174	0.161	0.878
LUAD	8 or 9 vs. 4 clones	0.264	-1.331	0.188
LUAD	10 or more vs. 4 clones	0.297	-1.215	0.275
LUAD	Age at diagnosis	22.962	3.134	0.196
LUAD	Low/high CNV abundance	0.024	-3.729	0.038
LUAD	MKI67	38.970	3.663	0.300
LUAD	% Lymphocytes	0.000	-9.200	0.106
LUAD	Pathologic stage	185.22(*)	5.222	2.98E-05
SKCM	1 or 2 vs. 3 clones	0.036	-3.337	0.121
SKCM	5 vs. 3 clones	0.019	-3.979	0.026
SKCM	6 or 7 vs. 3 clones	0.009	-4.722	0.016
SKCM	10 or more vs. 3 clones	0.093	-2.374	0.085
SKCM	Age at diagnosis	11.428	2.436	0.170
SKCM	Low/high CNV abundance	0.741	-0.300	0.945
SKCM	MKI67	0.002	-6.253	0.221
SKCM	% Lymphocytes	0.000	-43.821	0.043
SKCM	Pathologic stage	3.487	1.249	0.592
STAD	1 or 2 vs. 4 clones	0.341	-1.076	0.144
STAD	3 vs. 4 clones	0.638	-0.450	0.429
STAD	5 vs. 4 clones	0.401	-0.914	0.161
STAD	6 or 7 vs. 4 clones	0.483	-0.727	0.171
STAD	8 or 9 vs. 4 clones	0.767	-0.265	0.662
STAD	10 or more vs. 4 clones	0.436	-0.830	0.201
STAD	Age at diagnosis	4.596	1.525	0.266

STAD	Low/high CNV abundance	0.191	-1.653	0.232
STAD	% Lymphocytes	0.103(*)	-2.268	0.323
STAD	Grade	13.052	2.569	0.065
STAD	Pathologic stage	8.591	2.151	0.002
LUSC	3 vs. 4 clones	0.795	-0.230	0.786
LUSC	5 vs. 4 clones	0.560	-0.579	0.517
LUSC	6 or 7 vs. 4 clones	0.544	-0.609	0.439
LUSC	8 or 9 vs. 4 clones	0.647	-0.435	0.545
LUSC	Age at diagnosis	2.178	0.778	0.727
LUSC	Low/high CNV abundance	0.084	-2.477	0.099
LUSC	MKI67	16.344	2.794	0.435
LUSC	% Lymphocytes	1.025	0.025	0.990
LUSC	Pathologic stage	5.297	1.667	0.110

References

1. Sathirapongsasuti, J. F. *et al.* Exome sequencing-based copy-number variation and loss of heterozygosity detection: ExomeCNV. *Bioinforma. Oxf. Engl.* **27,** 2648–2654 (2011).

2. Cibulskis, K. *et al.* Sensitive detection of somatic point mutations in impure and heterogeneous cancer samples. *Nat. Biotechnol.* **31,** 213–219 (2013).

3. Roth, A. *et al.* JointSNVMix: a probabilistic model for accurate detection of somatic mutations in normal/tumour paired next-generation sequencing data. *Bioinforma. Oxf. Engl.* **28,** 907–913 (2012).

4. Andor, N., Harness, J. V., Müller, S., Mewes, H. W. & Petritsch, C. EXPANDS: expanding ploidy and allele frequency on nested subpopulations. *Bioinforma. Oxf. Engl.* **30,** 50–60 (2014).

5. Roth, A. *et al.* PyClone: statistical inference of clonal population structure in cancer. *Nat. Methods* **11,** 396–398 (2014).

6. Carpenter, A. E. *et al.* CellProfiler: image analysis software for identifying and quantifying cell phenotypes. *Genome Biol.* **7,** R100 (2006).

7. Yoshihara, K. *et al.* Inferring tumour purity and stromal and immune cell admixture from expression data. *Nat. Commun.* **4,** (2013).

8. Armitage, P. & Doll, R. The Age Distribution of Cancer and a Multi-stage Theory of Carcinogenesis. *Br. J. Cancer* **8,** 1 (1954).

9. Huang, D. W., Sherman, B. T. & Lempicki, R. A. Systematic and integrative analysis of large gene lists using DAVID bioinformatics resources. *Nat. Protoc.* **4,** 44–57 (2009).

10. Huang, D. W., Sherman, B. T. & Lempicki, R. A. Bioinformatics enrichment tools: paths toward the comprehensive functional analysis of large gene lists. *Nucleic Acids Res.* **37,** 1–13 (2009).